

CONVERGENCE OF REGULARIZED PARTICLE FILTERS FOR STOCHASTIC REACTION NETWORKS *

ZHOU FANG[†], ANKIT GUPTA[†], AND MUSTAFA KHAMMASH[†]

Abstract. Filtering for stochastic reaction networks (SRNs) is an important problem in systems/synthetic biology aiming to estimate the state of unobserved chemical species. A good solution to it can provide scientists valuable information about the hidden dynamic state and enable optimal feedback control. Usually, the model parameters need to be inferred simultaneously with state variables, and a conventional particle filter can fail to solve this problem accurately due to sample degeneracy. In this case, the regularized particle filter (RPF) is preferred to the conventional ones, as the RPF can mitigate sample degeneracy by perturbing particles with artificial noise. However, the artificial noise introduces an additional bias to the estimate, and, thus, it is questionable whether the RPF can provide reliable results for SRNs. In this paper, we aim to identify conditions under which the RPF converges to the exact filter in the filtering problem determined by a bimolecular network. First, we establish computationally efficient RPFs for SRNs on different scales using different dynamical models, including the continuous-time Markov process, tau-leaping model, and piecewise deterministic process. Then, by parameter sensitivity analyses, we show that the established RPFs converge to the exact filters if all reactions leading to an increase of the molecular population have linearly growing propensities and some other mild conditions are satisfied simultaneously. This ensures the performance of the RPF for a large class of SRNs, and several numerical examples are presented to illustrate our results.

Key words. Regularized particle filters, stochastic reaction networks, multiscale systems, filtering theory.

AMS subject classifications. 60J22, 62M20, 65C05, 92-08, 93E11.

1. Introduction. The development of fluorescence technologies [61] and modern microscopes [54, 57] in the past few decades has greatly improved scientists' ability to study various biological problems at the single-cell level [41]. For instance, researchers can now use fluorescent data to investigate the variability in single-cell gene expression [49], and the role of transcription factors in shaping bursty dynamics [50]. Despite these successes, a time-lapse microscope can only follow a few genes over time due to the limited availability of distinguishable reporters [41]; consequently, many chemical species in the cell are not directly tracked. This drawback greatly limits scientists' ability to further investigate and control the dynamical behaviors of single-cell systems. Consequently, it is of immediate interest to establish efficient stochastic filters that can accurately infer the unobserved species in an intracellular reaction system by partial observations.

The filtering theory that aims to calculate the posterior of hidden dynamic states given the time-course observation has been extensively developed in the past few decades. In the linear and Gaussian scenarios, the solution to the filtering problem is the well-known Kalman filter [33], which can be calculated exactly in a computationally efficient way. In contrast, the nonlinear and non-Gaussian systems usually lead to infinite-dimensional filters that cannot be calculated explicitly [5]. In this case, the particle filter (PF) originally introduced in [26] is the most effective method to numerically solve the filtering problem, which approximates the posterior by a population of weighted samples generated by importance sampling (from the target dynamics)

*Submitted to the editors DATE.

Funding: This work was funded by the Swiss National Science Foundation under grant number 182653.

[†]Department of Biosystems Science and Engineering, ETH Zurich, Mattenstrasse 26, 4058 Basel, Switzerland (zhou.fang@bsse.ethz.ch, ankit.gupta@bsse.ethz.ch, mustafa.khammash@bsse.ethz.ch)

and resampling [14]. So far, PFs have been successfully applied to biochemical reaction systems under different problem settings, e.g., the heat shock response system [40], metabolic dynamics [58], transcriptional switch models [31], multiscale reaction systems [17, 18], biochemical processes of noise-free observations [48]. Moreover, the method has been shown to outperform other stochastic filters (e.g., extended Kalman filters and unscented Kalman filter) in general situations [40].

Usually, an intracellular reaction system is modeled by a continuous-time Markov Chain, also known as the stochastic reaction network (SRN), due to low molecular counts [42]. Its dynamics can be exactly simulated by the Gillespie stochastic simulation algorithm [21, 22] or the next reaction method [19], whose computational complexity is proportional to the rate of the fastest reaction. Commonly, an SRN has a multiscale nature, meaning that the concentration levels of the involved species differ by several orders of magnitude, and so do the reaction rates. Consequently, the exact simulation of an intracellular reaction system can take an impractical amount of computational time, and the associated PF, as a simulation-based algorithm, can be computationally inefficient. Accelerating algorithms for SRNs include the linear noise approximation [56], chemical Langevin equation [23], tau-leaping algorithm [24, 8, 46], piecewise deterministic Markov process (PDMP) [34, 30, 11], etc., all of which reduce the computational complexity via approximating the firing of fast reactions by more tractable processes. (We refer interested readers to the literature [51] for a related discussion.) Inspired by these methods, researchers also proposed computationally efficient particle filters using linear noise approximations [52], chemical Langevin equations [40, 25], and PDMPs [18, 17, 31].

Another feature of intracellular reaction systems that needs to be considered is the large variability in model parameters from cell to cell, which suggests that model parameters should be inferred simultaneously with the state variables in the filtering problem. A common way to combine these two tasks together is to view the model parameters as additional states of the system and, then, to use the PF to infer the augmented state vector. In this situation, the conventional sequential importance resampling PF (SIRPF) suffers from sample degeneracy, meaning that the particle diversity in parameters drops dramatically over time, and, therefore, the particles fail to represent the posterior accurately. Good alternatives to SIRPFs include the resample-move method [20, 6] and the regularized particle filter (RPF) [39, 44], all of which mitigate sample degeneracy by perturbing particles with (additional) artificial noise and have been successful in various applications (see the aforementioned references). This methodology is easy to implement but has the drawback that it treats model parameters (which are fixed over time) as time-varying variables and, consequently, throws away some information about them [39]. In the finite particle population case, researchers still cannot quantify the bias introduced by the artificial noise in an RPF [36]. However, in the large-particle limit, the RPF has already been shown to converge to the exact filter if the artificial noise is weak and the transition kernel satisfies some regularity conditions, e.g., the globally Lipschitz continuity [13, Proposition 2.38], the mixing condition in the metric space [37], and the Lipschitz continuity of transition kernel’s derivatives [10].

Motivated by the above facts, we present in this paper a computationally efficient RPF for multiscale SRNs based on reduced dynamical models and identify conditions under which the performance of the established RPF is guaranteed. We note that the existing results about the convergence of RPFs cannot be directly applied to our problem. First, the globally Lipschitz condition of the transition kernel required in [13, Proposition 2.38] is too restrictive for SRNs that only a limited class of networks,

such as those having linear propensities or bounded trajectories, satisfy it. In addition, the discreteness of the state space of an SRN suggests that the mixing condition in the whole metric space [37] and the derivative related condition [10] can never hold. Instead, in this paper, we approach the problem by utilizing parameter sensitivity results in [27, 28, 29]. The rationale is that the parameter sensitivity can be used to quantify the effect of the artificial noise exerted to the model parameters; once we show that the error caused by artificial noise is small, the convergence of the RPF holds automatically. Following this idea, we show that the established RPF converges to the exact filter in probability, if all the reactions that lead to an increase of the molecule population have linearly growing propensities and some other mild conditions are satisfied simultaneously. The provided conditions are quite general, and they cover a large class of SRNs, including all mass-action networks in which only unimolecular reactions can lead to an increase of the total molecular population.

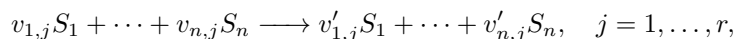
For the sake of simplicity, we only consider discrete-time observations in this paper. However, we conjecture that the obtained result can be naturally extended to the continuous-time observation case with mild modifications, as the parameter sensitivity analysis, the major technique used here, applies for continuous observations. Besides, compared with the SIRPF that we provided previously for multiscale SRNs in [17, 18], the RPF established in this paper has a relatively similar computational cost but a superior performance in inferring model parameters when the parameter uncertainty is large.

The rest of this paper is organized as follows. In Section 2, we briefly review the basics of SRNs and introduce the associated filtering problems. Then, by using different dynamical models, we establish computationally efficient RPFs for SRNs on different scales and provide several mild conditions that guarantee the performance of the established algorithm in the limit of large particles (see Section 3). When the particle population is finite, we also give a tuning rule for the hyperparameter (the intensity of artificial noise) so that a more precise estimate can be obtained. In Section 4, several numerical examples are presented to illustrate the effectiveness of the constructed RPF, particularly its superior performance to the SIRPF. Finally, Section 5 concludes this paper. To improve the readability of the paper, all the proofs are presented in the appendix.

2. Preliminary.

2.1. Notations. In this paper, we denote the natural filtered probability space by $(\Omega, \mathcal{F}, \{\mathcal{F}_t\}_{t \geq 0}, \mathbb{P})$, where Ω is the sample space, \mathcal{F} is the σ -algebra, $\{\mathcal{F}_t\}_{t \geq 0}$ is the filtration, and \mathbb{P} is the natural probability. Also, we term $\mathbb{N}_{>0}$ as the set of positive integers, \mathbb{R}^n with n being a positive integer as the space of n -dimensional real vectors, $\|\cdot\|_2$ as the Euclidean norm, and $|\cdot|$ as the absolute value notation. For any positive integer n and any $t > 0$, we term $\mathbb{D}_{\mathbb{R}^n}[0, t]$ as the Skorokhod space that consists of all \mathbb{R}^n valued cadlag functions on $[0, t]$.

2.2. Stochastic reaction networks. In this paper, we consider an intracellular reaction system that consists of n chemical species (S_1, \dots, S_n) and r reactions:



where $v_{i,j}$ and $v'_{i,j}$ are stoichiometric coefficients representing numbers of molecules consumed and produced in each reaction. We term $X(t) = (X_1(t), X_2(t), \dots, X_n(t))^T$ as the vector of copy numbers of these species at time t . Due to the small number of

reactant molecules, an intracellular reaction system is usually model by a stochastic model, called the continuous-time Markov chain, whose dynamics are described by [3]

$$X(t) = X(0) + \sum_{j=1}^r \zeta_j R_j \left(\int_0^t \lambda_j(k, X(s)) ds \right)$$

where $\zeta_j \triangleq v'_j - v_j$ (for $j = 1, \dots, r$), $R_j(t)$ are independent unit rate Poisson processes, $k = (k_1, \dots, k_{\tilde{r}})^\top$ is an \tilde{r} -dimensional vector of model parameters, and $\lambda_j(\kappa, x)$ are propensities indicating the speed of reaction firing. The most common propensity in chemistry and biology is the mass-action type, where $\lambda_j(\kappa, x) = k_j \prod_{i=1}^m \frac{x_i!}{(x_i - v_{i,j})!} \mathbb{1}_{\{x_i \geq v_{i,j}\}}$ with $\mathbb{1}_{\{\cdot\}}$ the indicator function. In the literature, the above model describing the dynamics of intracellular reaction systems is termed as a stochastic reaction network (SRN) due to the stochasticity of the dynamics and the network structure of the chemical reactions.

Usually, an SRN encountered in systems biology is multiscale in nature [34], meaning that different species vary a lot in abundance, and so do reaction rates. Following [34], these quantities at different scales can be normalized as follows. Let N be a scaling factor, the parameter α_i the abundance factor of the i -th species such that $X_i^N(t) \triangleq N^{-\alpha_i} X_i(t) = O(1)$, and the parameter β_j the magnitude of k_j such that $k'_j \triangleq k_j N^{-\beta_j} = O(1)$. Similarly, we term ρ_j as the timescale of the j -th reaction such that $\lambda_j^N(\mathcal{K}, X^N(t)) \triangleq N^{-\rho_j} \lambda_j(k, X(t)) = O(1)$ where $\mathcal{K} \triangleq (k'_1, \dots, k'_{\tilde{r}})^\top$. Particularly, in the mass-action kinetics, these coefficients satisfy $\rho_j = \beta_j + \sum_{i=1}^m v_{i,j} \alpha_i$. Finally, by denoting $X^{N,\gamma}(t) \triangleq X^N(tN^\gamma)$ with γ the timescale of interest, we can re-express the dynamics as

$$(2.1) \quad X^{N,\gamma}(t) = X^{N,\gamma}(0) + \sum_{j=1}^r \Lambda^N \zeta_j R_j \left(\int_0^t N^{\gamma+\rho_j} \lambda_j^N(\mathcal{K}, X^{N,\gamma}(s)) ds \right)$$

where $\Lambda^N \triangleq \text{diag}(N^{-\alpha_1}, \dots, N^{-\alpha_s})$, and all terms but Λ^N and $N^{\gamma+\rho_j}$ are in the order of $O(1)$. In the sequel, we study the SRN in the normalized coordinate. Also, for simplicity, we concern ourselves with the fastest timescale of the system, i.e., $\gamma_1 \triangleq \min_i \{ \alpha_i - \max_{j \in \{v_{i,j} \neq 0\}} \rho_j \}$, on which the system evolves at the rate of $\mathcal{O}(1)$.

2.3. Filtering problems for SRNs. Stochastic filtering for SRNs aims to infer hidden dynamic states of an SRN from partial observations of the system. Usually, we need to simultaneously estimate the model parameter \mathcal{K} in this filtering problem due to the uncertainty of \mathcal{K} . In this paper, we suppose $(\mathcal{K}, X^N(0))$ to have a known prior distribution.

For the observation, we assume that m channels of light intensity signals, denoted by $Y^{N,\gamma_1}(\cdot)$, can be observed (with a microscope for instance) and satisfy

$$Y^{N,\gamma_1}(t_i) = h(X^{N,\gamma_1}(t_i)) + W(t_i) \quad \forall i \in \mathbb{N}_{>0},$$

where $\{t_i\}_{i \in \mathbb{N}_{>0}}$ is a strictly increasing sequence of time points at which the observation is collected, h is an m -dimensional bounded Lipschitz continuous function indicating the relation between the observation and the SRN, and $\{W_\ell(t_i)\}_{i \in \mathbb{N}_{>0}}$ are independent m -variate standard Gaussian random variables. Usually, the dimension of the observation vector is much less than that of the state vector, meaning that only a part of the system information is detected. Besides, we assume that the observation noise is independent of the dynamical system (2.1), i.e., $\{W_\ell(t_i)\}_{i \in \mathbb{N}_{>0}}$ are

independent of Poisson processes $R_j(\cdot)$ ($j = 1, \dots, r$), system parameters \mathcal{K} , and the initial condition $X^N(0)$. In the sequel, we term $\mathcal{Y}_{t_i}^{N, \gamma_1}$ as the σ -algebra generated by observations up to the time t_i .

In the filtering problem, the standard object to study is the conditional distribution process $\{\pi_{t_i}^{N, \gamma_1}\}_{i \in \mathbb{N}_{>0}}$ given by $\pi_{t_i}^{N, \gamma_1}(\phi) \triangleq \mathbb{E}_{\mathbb{P}} \left[\phi(\mathcal{K}, X^{N, \gamma_1}(t_i)) \mid \mathcal{Y}_{t_i}^{N, \gamma_1} \right]$ for any measurable function $\phi: \mathbb{R}^{\bar{r}} \times \mathbb{R}^n \rightarrow \mathbb{R}$. This conditional distribution process satisfies the following relations [5, Proposition 10.6]

$$(2.2) \quad p_{t_i}^{N, \gamma_1}(A) = \int_{z \in \mathbb{R}^{\bar{r}} \times \mathbb{R}^n} K_{t_i - t_{i-1}}^{N, \gamma_1}(z, A) \pi_{t_{i-1}}^{N, \gamma_1}(dz), \quad \forall A \subset \mathbb{R}^{\bar{r}} \times \mathbb{R}^n \text{ and } \forall i \in \mathbb{N}_{>0},$$

$$(2.3) \quad \frac{d\pi_{t_i}^{N, \gamma_1}}{dp_{t_i}^{N, \gamma_1}} = \frac{\ell_{Y^{N, \gamma_1}(t_i)}}{p_{t_i}^{N, \gamma_1}(\ell_{Y^{N, \gamma_1}(t_i)})}, \quad \forall i \in \mathbb{N}_{>0},$$

where $t_0 = 0$, $\pi_{t_0}^{N, \gamma_1}$ is the initial distribution, $K_t^{N, \gamma_1}(z, A)$ is the transition kernel of the system (2.1) being equal to $\mathbb{P}((\mathcal{K}, X^{N, \gamma_1}(t)) \in A \mid (\mathcal{K}, X^{N, \gamma_1}(0)) = z)$, and $\ell_y(\kappa, x) \triangleq \mathbb{P}(Y^{N, \gamma_1}(t_i) = y \mid X^{N, \gamma_1}(t_1) = x)$ is the likelihood function. Here, equation (2.2) can be interpreted as a prediction step where one estimates hidden dynamic states at t_i using observations up to the previous time points, and (2.3) is an adjustment step where the conditional distribution is obtained by reweighing the prediction according to the new observation. Usually, the above equations cannot be solved explicitly; therefore, we intend to establish efficient particle filtering algorithms that can quickly and accurately solve these filtering problems.

2.4. Model reduction for SRNs. The dynamics of an SRN is a continuous-time Markov chain (CTMC) which can be exactly simulated using the Gillespie stochastic simulation algorithm [21, 22] or the next reaction method [19]. The computational complexity of these exact simulation algorithms is inversely proportional to the fastest timescale of reactions; therefore, these algorithms can only be computationally efficient for those SRNs having no fast reaction (i.e., the maximum $N^{\gamma_1 + \rho_j}$ is small), otherwise they take an impractical amount of computational time to simulate systems. This fact can also have an adverse effect on particle filtering, as it is a simulation-based method (more details are illustrated in the next section). To accelerate the simulation, a few algorithms have been invented for systems on different scales. In the following, we review two well-known reduced models, the tau-leaping model and the piecewise deterministic Markov process (PDMP).

2.4.1. Tau-leaping. The tau-leaping method is a stochastic analog to the Euler method for ODEs, where the algorithm changes the value of the propensities periodically over time rather than instantaneously after each jump event. Since the propensity is updated much less frequently in this method than in the exact simulation method, the tau-leaping algorithm consumes much less computational time to simulate the system. At the timescale γ_1 , the tau-leaping algorithm can be expressed as

$$(2.4) \quad X_{\tau}^{N, \gamma_1}(t) = X^N(0) + \sum_{j=1}^r \Lambda^N \zeta_j R_j \left(\sum_{i=0}^{\infty} (\tau_{i+1} \wedge t - \tau_i \wedge t) N^{\gamma_1 + \rho_j} \lambda_j^N(\mathcal{K}, X_{\tau}^{N, \gamma_1}(\tau_i)) \right)$$

where $X_\tau^{N,\gamma_1}(t)$ is the state vector, and $\{\tau_i\}_{i \in \mathbb{N}}$ is an increasing sequence of time points at which propensities are updated. Equivalently, it can also be written by

$$X_\tau^{N,\gamma_1}(\tau_{i+1}) = X_\tau^{N,\gamma_1}(\tau_i) + \sum_{j=1}^r \Lambda^N \zeta_j \mathcal{P}_{j,i}$$

where $\mathcal{P}_{j,i}$ are independent Poisson-distributed random variables with mean $(\tau_{i+1} - \tau_i) N^{\gamma_1 + \rho_j} \lambda_j^N(\mathcal{K}, X_\tau^{N,\gamma_1}(\tau_i))$. For simplicity, in this paper, we consider the case where the grid $\{\tau_i\}_{i \in \mathbb{N}}$ is deterministic and contains all the observation times. Usually, the leaping time should be short enough so that the normalized propensity will not change much during $[\tau_i, \tau_{i+1})$. Also, it should be greater than the timescale of the fastest reaction so that it leaps over several reaction firing events and, thus, is faster than the exact simulation method. Often, the tau-leaping algorithm is applied to systems containing $10^2 \sim 10^3$ molecules [32] (in other words, the maximum $N^{\gamma_1 + \rho_j}$ is $\mathcal{O}(10^2 \sim 10^3)$).

In this paper, we only consider applying the tau-leaping algorithm to the system where the following assumptions hold.

ASSUMPTION 2.1 (Nonnegativity of the tau-leaping algorithm). *Denote $|\tau| \triangleq \max_i(\tau_{i+1} - \tau_i)$. Then, for any $t > 0$ and any $|\tau| > 0$, the state $X_\tau^{N,\gamma_1}(t)$ is always nonnegative.*

ASSUMPTION 2.2 (Consistency of the tau-leaping algorithm). *For any fixed \mathcal{K} , there holds $X_\tau^{N,\gamma_1}(\cdot) \xrightarrow{|\tau| \rightarrow 0} X^{N,\gamma_1}(\cdot)$ on any interval $T > 0$, in the sense of the Skorokhod topology.*

In general, the above two properties assumed for the tau-leaping method are essential and non-restrictive. The nonnegativity assumption ensures the algorithm to generate reasonable trajectories that evolve in the nonnegative orthant, and this property can be achieved by wisely designing the grid $\{\tau_i\}_{i \in \mathbb{N}}$ (see [1]). The consistency assumption states that the tau-leaping algorithm is accurate (in the weak sense) in simulating the target system when the coarseness of the time-discretization scheme is small enough. A few sufficient conditions for the consistency assumption have been provided in the literature [2, 38, 47] (for bounded processes) and [45] (for unbounded processes).

2.4.2. Piecewise deterministic Markov Processes (PDMP). For a system having an extremely large scaling factor N , the PDMP is a favorable approximate model, where the firing events of fast reactions are approximated by continuous processes, and those slow reactions are kept as what they are. Specifically, for fast reactions ($j \in \{\gamma_1 + \rho_j > 0\}$), this method utilizes Poisson's law of large numbers to approximate the reaction firing events by continuous processes, i.e.,

$$N^{-\gamma_1 - \rho_j} \zeta_j R_j \left(\int_0^t N^{\gamma_1 + \rho_j} \lambda_j^N(\mathcal{K}, X^{N,\gamma_1}(s)) ds \right) \approx D^{\gamma_1 + \rho_j} \zeta_j \left(\int_0^t \lambda_j'(\mathcal{K}, X^{\gamma_1}(s)) ds \right)$$

where $\lambda_j'(\kappa, x) = \lim_{N \rightarrow +\infty} \lambda_j^N(\kappa, x)$, $X^{\gamma_1}(\cdot)$ is the limit process of $X^{N,\gamma_1}(\cdot)$, and $D^{\tilde{\alpha}} \triangleq \text{diag}(\mathbb{1}_{\{\alpha_1 = \tilde{\alpha}\}}, \dots, \mathbb{1}_{\{\alpha_n = \tilde{\alpha}\}})$ indicates whether a species has the abundance fac-

tor $\tilde{\alpha}$. In this regard, the reduced model can be written by [34]

$$(2.5) \quad X^{\gamma_1}(t) = \lim_{N \rightarrow \infty} X^N(0) + \sum_{j: \gamma_1 + \rho_j > 0} D^{\gamma_1 + \rho_j} \zeta_j \left(\int_0^t \lambda'_j(\mathcal{K}, X^{\gamma_1}(s)) ds \right) \\ + \sum_{j: \gamma_1 + \rho_j = 0} D^0 \zeta_j R_j \left(\int_0^t \lambda'_j(\mathcal{K}, X^{\gamma_1}(s)) ds \right)$$

where $\lim_{N \rightarrow \infty} X^N(0)$ is assumed to exist. Since the above Markov process is deterministic between two neighboring jumping times, it is named the piecewise deterministic Markov process (PDMP). For a slower timescale, such a reduced model can also be constructed in the same spirit if some fast species are first eliminated by quasi-stationary assumption. A systematic procedure to construct a hierarchy of PDMPs representing dynamics in different timescales can be found in the literature [34].

When N is large, the simulation time of PDMPs is much less than that of the full model, because the PDMP avoids the exact simulation of fast reactions, and those continuous processes that approximate the firing events of fast reactions can be computed efficiently by the Euler method. Detailed algorithms to simulate PDMPs have been provided in the literature [11, 15, 30]. The accuracy of the PDMP is ensured by the following proposition.

ASSUMPTION 2.3. $\lim_{N \rightarrow \infty} X^N(0)$ exists a.s., and $\lim_{N \rightarrow \infty} X_i^N(0) > 0$ if $\alpha_i > 0$.

PROPOSITION 2.4 (Adapted from [34]). For any fixed \mathcal{K} , if Assumption 2.3 holds, and $X^{N, \gamma_1}(t)$ (for all $N \in \mathbb{N}_{>0}$) and $X^{\gamma_1}(t)$ are almost surely non-explosive, then $X^{N, \gamma_1}(\cdot) \xrightarrow{N \rightarrow \infty} X^{\gamma_1}(\cdot)$ in the sense of the Skorokhod topology on any finite time interval $[0, T]$.

2.4.3. Working ranges of different simulation algorithms. The working ranges of the aforementioned simulation algorithms are quite different. When all reactions fire at the rate of $\mathcal{O}(1 \sim 10)$ (i.e., all $N^{\gamma_1 + \rho_j}$ are $\mathcal{O}(1 \sim 10)$), the exact simulation algorithms for the CTMC are recommended, as they are perfectly accurate and computationally efficient in this case. The tau-leaping algorithm is usually applied to systems where the fastest reaction fires at the rate of $\mathcal{O}(10^2 \sim 10^3)$; in this scenario, the tau-leaping algorithm can be much faster than the exact simulation method while still capturing key behaviors of the system. Finally, when the scaling factor N is sufficiently large, the PDMP method is preferred to the others, because in this situation the randomness of fast reaction firing is averaged out due to the law of large numbers.

There is still one situation excluded here, that some reactions fire at extremely fast rates (e.g., $\mathcal{O}(10^4)$), but some others fire at the rate of $\mathcal{O}(10^2 \sim 10^3)$. In this case, the PDMP model fails to capture key behaviors of the system, as there is still randomness in those reactions on medium timescales. On the other hand, the tau-leaping method is slow in this situation, because it needs to frequently generate Poisson random variables of large means. Instead, the diffusion approximation is recommended for these systems, where the firing of a medium timescale reaction is approximated by a diffusion process. Since this algorithm just needs to generate Gaussian random variables, the computational cost is low; moreover, its accuracy is higher than that of the PDMP [35]. However, in this paper, we do not consider this type of approximation due to the difficulties in the analysis (particularly the parameter sensitivity analysis of this reduced model).

3. Regularized particle filter (RPF) for SRNs.

3.1. Constructing RPFs for SRNs on different scales. Usually, the conditional distribution of an SRN cannot be computed explicitly due to the nonlinearity of the dynamics. Therefore, we apply particle filters to the associated filtering problem. The key idea of the particle filtering (also known as the sequential Monte Carlo method [26]) is to approximate the posterior by a number of weighted trajectories sampled from the distribution of the target system. A detailed particle filtering algorithm is provided in [Algorithm 3.1](#). Specifically, the sampling step in [Algorithm 3.1](#) mimics the recursive formulas (2.2) (the prediction step) and (2.3) (the adjustment step), in which weighted particles are generated to represent the conditional distribution. The resampling step is executed to remove insignificant particles and, therefore, mitigate long-term weight degeneracy at the cost of adding additional noise at the current step [14]. In this paper, we use the residual resampling, as it introduces the minimum noise among all resampling methods [5, Exerice 9.1]. Finally, particles are perturbed by artificial noise so that the particle diversity improves, and the sample degeneracy meaning that all particles become identical can be avoided. Such a particle filtering algorithm with an artificial evolution step is called a regularized particle filter (RPF); if the artificial evolution is not executed, then this algorithm is called a sequential importance resampling particle filter (SIRPF).

Algorithm 3.1 Regularized particle filter [44]

- 1: Input observations $\{Y(t_i)\}_{i \in \mathbb{N}}$, a dynamical model, and the initial distribution.
 - 2: *Initialization*: Sample M particles $(\bar{\kappa}_1(0), \bar{x}_1(0)), \dots, (\bar{\kappa}_M(0), \bar{x}_M(0))$; set $i = 1$ and $t_0 = 0$.
 - 3: **while** t_i does not exceed the terminal time of the observations **do**
 - 4: *Sampling*: simulate $x_j(\cdot)$ ($j = 1, \dots, M$) from time t_{i-1} to t_i according to the dynamical model with parameters $\bar{\kappa}_j(t_{i-1})$ and initial conditions $\bar{x}_j(t_{i-1})$; Set $\kappa_j(t_i) = \bar{\kappa}_j(t_{i-1})$; Calculate weights $w_j(t_i) \propto \ell_{Y^N, \gamma(t_i)}(\kappa_j(t_i), x_j(t_i))$.
 - 5: *Output the filter*: $\bar{\pi}_{M, t_i}(\phi) = \sum_{j=1}^M w_j(t_i) \phi(\kappa_j, x_j(t_i))$.
 - 6: *Resampling*: Resample $\{w_j(t_i), (\kappa_j(t_i), x_j(t_i))\}_j$ to obtain M equally weighted samples $\{1/M, (\hat{\kappa}_j(t_i), \bar{x}_j(t_i))\}_j$. (Residual resampling is applied)
 - 7: *Artificial evolution*: sample $\bar{\kappa}_j(t_i)$ from a kernel $\eta_M(\cdot | \hat{\kappa}_j(t_i))$.
 - 8: **end while**
-

Conventionally, in the sampling step, particles are obtained by simulating the full dynamical model of the system. However, it is not plausible for SRNs, especially the multiscale ones, where the exact simulation of (2.1) can take an impractical amount of computational time. Instead, for SRNs on different scales, we utilize different dynamical models in the sampling step so that the filter is computationally efficient. The specific construction of such RPFs is as follows.

DEFINITION 3.1 (RPFs for SRNs on different scales).

- If all reactions fire at the rate of $\mathcal{O}(1 \sim 10)$ (i.e., all $N^{\gamma_1 + \rho_j}$ are $\mathcal{O}(1 \sim 10)$), then we build the filter by utilizing exact simulation algorithms in the sampling step. We denote such a RPF by $\bar{\pi}_{M, t_i}^{N, \gamma_1}$.
- If the fastest reaction fires at the rate of $\mathcal{O}(10^2 \sim 10^3)$, then we use the tau-leaping method in the sampling step. We denote such a RPF by $\bar{\pi}_{M, t_i}^{N, \gamma_1, \tau}$.
- If N is extremely large, we use the PDMP in the sampling step. We denote such a RPF by $\bar{\pi}_{M, t_i}^{N, \gamma_1, H}$. (Here, H stands for hybrid approximations. This

filter has dependence on N because the observation $Y^{N,\gamma_1}(\cdot)$ is input into the algorithm.)

Another important factor for the RPF is the artificial noise used in the artificial evolution step. Though this noise can mitigate sample degeneracy, it also introduces a bias to the estimate. Therefore, if the kernel η_M is not carefully chosen, the RPF can yield a very inaccurate estimate of the conditional distribution. In this paper, we design the kernel η_M according to the following assumptions so that the intensity of the artificial noise is contained.

ASSUMPTION 3.2.

- \mathcal{K} 's prior distribution has a compact convex support. We denote it by Θ .
- We term \mathcal{V} as the covariance matrix of \mathcal{K} at the initial time. Then, for any $M > 0$ and $\kappa \in \Theta$, the kernel $\eta_M(\cdot|\kappa)$ satisfies

$$\eta_M(\tilde{\kappa}|\kappa) \propto \mathbb{1}_{\{\tilde{\kappa} \in \Theta\}} \mathcal{N}(\tilde{\kappa} | \kappa, C_\eta^2 \mathcal{V} / M) \quad \forall \tilde{\kappa} \in \mathbb{R}^{\tilde{r}},$$

where C_η is a predetermined positive constant, and $\mathcal{N}(\cdot | \kappa, C_\eta^2 \mathcal{V} / M)$ is a Gaussian kernel with κ mean and $C_\eta^2 \mathcal{V} / M$ covariance matrix.

In general, the above assumption suggests that the artificial evolution keeps particles in the support of the prior distribution, and the artificial noise is in the order of $O(M^{-1/2})$.

Remark 3.3. In references [39, 40], there is an alternative choice of the artificial noise where $\eta_M(\tilde{\kappa}|\kappa) = \mathcal{N}(\tilde{\kappa} | a\kappa + (1-a)\mu_t, (1-a)C_\eta^2 \mathcal{V}_t / M)$ with μ_t and \mathcal{V}_t the mean and covariance matrix of particles $\{\hat{k}_j(t_i)\}_{1 \leq j \leq M}$ and ‘ a ’ a constant in $[0, 1]$. Compared with our setting, this one can adjust the artificial noise intensity dynamically according to the particle distribution, and, moreover, the associated filter can avoid “variance inflation” [39], meaning that the artificial evolution in its filter does not change the particle variance. However, we think that variance inflation is beneficial, and with the method in [39, 40], the RPF can only delay sample degeneracy but never fully solve it. The reasons are as follows. With more observations collected, the exact posterior of the model parameter becomes narrower, and the variance of the particles corresponds to \mathcal{K} inclines to decay dramatically over time. Since the method in [39, 40] avoids variance inflation, its particle variance decays strictly over time and finally degenerates to zero; in other words, the particles $\{k_j(t_i)\}_{1 \leq j \leq M}$ collapse into a single point in the end. Ideally, the point should be close to the maximum of the posterior. However, due to the randomness, this ideal case can rarely happen, and, consequently, sample degeneracy arises. In contrast, the RPF satisfying [Assumption 3.2](#) can greatly improve the particle variance (when it is too small) due to the constant covariance matrix of the artificial noise and, therefore, can fully solve the sample degeneracy problem.

Another fact to support our choice of artificial noise is that in reality the model parameters fluctuate dynamically in individual living cells due to environmental changes and the cell cycle [49]. This requires the algorithm to generate diverse particles even if the exact posterior is very narrow. Again, due to the constant covariance matrix of the artificial noise, our framework meets this requirement.

Remark 3.4. Compared with our previous work [17, 18], where an SIRPF was established for SRNs based on the PDMP, this paper constructs filters using one more reduced model, the tau-leaping method. More importantly, the RPF constructed in this paper involves an artificial evolution step, which can mitigate sample degeneracy

and make the filter perform better when the parameter uncertainty is large. In the next section, we will illustrate this point using several numerical examples.

3.2. Convergence of RPFs. In this subsection, we investigate conditions under which the established RPFs can provide reliable estimates of the hidden dynamic states and model parameters in the limit of large particles. In the literature [13, 37, 10], a few conditions have been proposed to guarantee the convergence of RPFs; however, none of them can be directly applied to our setting for the following reasons.

Remark 3.5. It has been shown that an RPF converges to the exact filter if the artificial noise is weak and the transition kernel satisfies some regularity conditions, e.g., the globally Lipschitz continuity [13, Proposition 2.38], the mixing condition in the metric space [37], and the Lipschitz continuity of transition kernel's derivatives [10]. For an SRN, the globally Lipschitz continuity of the transition kernel is very restrictive; it usually requires the propensities to be Lipschitz continuous (e.g., linear propensities), or the trajectory to evolve in a bounded region. In addition, the discrete state space of an SRN invalidates the mixing condition in the whole metric space [37] and the derivative related condition in [10].

In this paper, we approach this problem in an alternative way. Note that when the intensity of the artificial noise is zero, the constructed RPF degenerates to an SIRPF, and its convergence has been shown in part in our previous work [17]. Therefore, the key to proving the convergence of the established RPFs lies in estimating the bias introduced by the artificial evolution and showing it to vanish as particle population tends to infinity. This corresponds to calculating the parameter sensitivity for SRNs, as the artificial noise only perturbs the model parameter part of the particles. Fortunately, neat expressions for this parameter sensitivity function have been provided in the literature [27, 28, 29], by which we can easily analyze the bias of interest. Finally, through some technical analyses, we can show that both the parameter sensitivity and the state vector grow mildly under some weak conditions, and, consequently, the constructed RPF is convergent in probability to the exact filter. More detailed discussions about it are presented in the Appendix.

We now specify a few assumptions needed in our main results. In Remark 3.9, we illustrate that such conditions are so mild that they cover a large class of SRNs.

ASSUMPTION 3.6.

- All the propensities $\lambda_j^N(\kappa, x)$ are twice differentiable with respect to κ . Moreover, there exist positive constants $C_{\lambda,1}$ and q such that

$$\max \left\{ |\lambda_j^N(\kappa, x)|, \left\| \frac{\partial \lambda_j^N(\kappa, x)}{\partial \kappa} \right\|_2, \left\| \frac{\partial^2 \lambda_j^N(\kappa, x)}{\partial \kappa^2} \right\|_2 \right\} \leq C_{\lambda,1} (1 + \|x\|_2^q)$$

for any $N > 0$, $j \in \{1, \dots, r\}$, $\kappa \in \Theta$, and $x \in \mathbb{R}_{\geq 0}^n$.

- For any $N > 0$ and $j \in \{1, \dots, r\}$, if $\lambda_j^N(\kappa, x) > 0$, then $x + \Lambda^N \zeta_j$ has no negative component.
- For any $p > 0$, there exists a constant $C_{0,p}$ such that $\mathbb{E} [\|X^N(0)\|_2^p] \leq C_{0,p}$
- There exists a positive constant $C_{\lambda,2}$ such that for any N and j satisfying $\bar{1}^\top \Lambda^N \zeta_j > 0$ ($\bar{1}$ is the all-one vector) there holds

$$\lambda_j^N(\kappa, x) \leq C_{\lambda,2} (1 + \|x\|_2) \quad \forall (\kappa, x) \in \Theta \times \mathbb{R}_{\geq 0}^n.$$

In other words, the propensity of the reaction that leads to an increase of the total population has at most a linear growth rate with the state argument.

ASSUMPTION 3.7. For any reaction j and parameter $\kappa \in \Theta$, the convergence $\lambda_j^N(\kappa, \cdot) \rightarrow \lambda_j'(\kappa, \cdot)$ (as $N \rightarrow \infty$) holds uniformly over compact sets. The same is true for derivatives $\frac{\partial \lambda_j^N(\kappa, \cdot)}{\partial \kappa} \rightarrow \frac{\partial \lambda_j'(\kappa, \cdot)}{\partial \kappa}$ and $\frac{\partial \lambda_j^N(\kappa, \cdot)}{\partial x} \rightarrow \frac{\partial \lambda_j'(\kappa, \cdot)}{\partial x}$.

Then, we present the main result of this paper, which states that the constructed RPFs can be very close to the exact filter when the particle population is large.

THEOREM 3.8. Assume that [Assumption 3.2](#) and [Assumption 3.6](#) hold. Also, we suppose the test function $\phi : \Theta \times \mathbb{R}_{\geq 0}^n \rightarrow \mathbb{R}$ to be bounded, continuous, and continuously differentiable in the first m -coordinates and satisfy

$$(3.1) \quad \left\| \frac{\partial \phi(\kappa, x)}{\partial \kappa} \right\|_2 \leq C_\phi (1 + \|x\|_2^q) \quad \forall (\kappa, x) \in \Theta \times \mathbb{R}_{\geq 0}^n,$$

where C_ϕ is a predetermined constant, and q is the same as that in [Assumption 3.6](#). Then, the following results for the constructed RPFs hold for any $i \in \mathbb{N}_{>0}$.

- $\lim_{M \rightarrow \infty} \mathbb{E} \left[\left| \bar{\pi}_{M, t_i}^{N, \gamma_1}(\phi) - \pi_{t_i}^{N, \gamma_1}(\phi) \right|^2 \right] = 0$ for any scaling factor N , where $\bar{\pi}_{M, t_i}^{N, \gamma_1}(\phi)$ is the filter built on exact simulation algorithms, and $\pi_{t_i}^{N, \gamma_1}(\phi)$ is the exact filter.
- If, moreover, [Assumption 2.1](#) and [Assumption 2.2](#) hold, then there is the relation $\lim_{M \rightarrow \infty} \lim_{|\tau| \rightarrow 0} \mathbb{E} \left[\left| \bar{\pi}_{M, t_i}^{N, \gamma_1, \tau}(\phi) - \pi_{t_i}^{N, \gamma_1}(\phi) \right|^2 \right] = 0$ for any N , where $\bar{\pi}_{M, t_i}^{N, \gamma_1, \tau}(\phi)$ is the filter built on the tau-leaping method.
- If [Assumption 2.3](#) and [Assumption 3.7](#) also hold, then there is the relation $\lim_{M \rightarrow \infty} \lim_{N \rightarrow +\infty} \mathbb{E} \left[\left| \bar{\pi}_{M, t_i}^{N, \gamma_1, H}(\phi) - \pi_{t_i}^{N, \gamma_1}(\phi) \right|^2 \right] = 0$, where $\bar{\pi}_{M, t_i}^{N, \gamma_1, H}(\phi)$ is the filter built on the PDMP model.

Proof. The proof is shown in the appendix. \square

Remark 3.9. The conditions required in the above theorem are not restrictive. [Assumption 2.1](#), [Assumption 2.2](#), and [Assumption 3.2](#) can be easily achieved by properly designing the tau-leaping algorithm and the RPF. [Assumption 2.3](#) and [Assumption 3.7](#) are concerned with the well-definiteness of the PDMP, which are reasonable to assume for those systems where the PDMP has already been successfully applied for simulation. For [Assumption 3.6](#), the first claim (the polynomial growth rate of the propensity) is satisfied in most SRNs considered in the existing literature (following the mass-action kinetics or the Hill-type dynamics); the second claim is nothing but ensuring the state vector to be nonnegative; the third requires all moments of initial conditions to be finite, which is natural in biology. The last claim in [Assumption 3.6](#) indicates that all reactions that lead to an increase of the molecular population have linearly growing propensities. Though the last one is not as weak as other assumptions, it still includes a lot of SRNs in systems biology, e.g., the simple birth-death model, the antithetic integral controller that interconnects to linear networks (see [\[7, 4\]](#) for antithetic integral controllers), and all mass-action networks where only unimolecular reactions can lead to an increase of the total molecular population. In summary, the conditions required in [Theorem 3.8](#) are quite mild, and the proposed RPFs work for a large class of SRNs.

3.3. Hyperparameter tuning. In the finite particle population case, the hyperparameter C_η , which depicts the intensity of the noise in artificial evolution (see [Assumption 3.2](#)), has a significant influence on the performance of the established

filter and, therefore, needs to be properly trained in advance. Intuitively, this hyperparameter tuning task is an exploration-exploitation trade-off: by increasing the hyperparameter C_η , the RPF can explore a broad region of the parameter space and have a higher chance to discover all regions of high posterior, but at the cost of missing some knowledge conveyed in the current particles.

To optimize the hyperparameter, we generate a large number of simulated trajectories, $\{(\tilde{\kappa}_\ell, \tilde{x}_\ell(\cdot), \tilde{y}_\ell(\cdot))\}$, where $(\tilde{\kappa}_\ell, \tilde{x}_\ell(0))$ are sampled from the prior of $(\mathcal{K}, X^N(0))$, $x_\ell(\cdot)$ is the simulated trajectory of the considered SRN, and $y_\ell(\cdot)$ is the simulated observation. A good C_η should make the associated particle filter close to the exact filter when applied to the simulated data. However, this criterion cannot be directly used to optimize C_η as the exact filter is unavailable.

Alternatively, we train the hyperparameter by the accuracy of the inferred parameters and the diversity of particles. This strategy first requires the parameter identifiability assumption meaning that given long-time observations, the posterior of the model parameter is densely distributed around the true value. This assumption is not very restrictive; usually, it can be checked by the frequency spectrum [53] and achieved by optimal experimental design [16]. According to the parameter identifiability, the accuracy of the RPF can be evaluated by the distance between the inferred model parameter (by the RPF) and the exact parameter. As the true value of the model parameter is known in the simulated data, we can easily apply this rule to training the filter. In addition, particle diversity in model parameters should also be considered in hyperparameter tuning, and we evaluate it by the entropy of the particles $(\{\kappa_j\}_{j=1,\dots,M})$. To describe particle diversity more accurately, we truncate the value of particles to four decimal places, so that two particles in close distance are regarded as identical ones. In conclusion, the optimal hyperparameter, denoted by C_η^* , which balances accuracy and diversity, can be obtained by solving the following optimization problem:

(3.2)

$$C_\eta^* = \arg \min_{C_\eta > 0} \sum_{\ell} \mathbb{E} \left[\bar{\pi}_{M,t_L,C_\eta} \left(\frac{\|\kappa - \tilde{\kappa}_\ell\|_2^2}{\|\tilde{\kappa}_\ell\|_2^2} \right) + \frac{1}{\exp(\mathcal{E}_{\pi_{M,t_L,C_\eta}})} \middle| Y^{N,\gamma_1}(t_i) = \tilde{y}_\ell(t_i), \forall t_i \leq t_L \right],$$

where t_L is a large time point, $\bar{\pi}_{M,t_L,C_\eta}$ represents the RPF established in Definition 3.1 with the hyperparameter C_η , and $\mathcal{E}_{\pi_{M,t_L,C_\eta}}$ is the entropy of the particles $\{\tilde{\kappa}_j\}_{j=1,\dots,M}$ at the time t_L . In this formula, the term $\bar{\pi}_{M,t_L,C_\eta} (\|\kappa - \tilde{\kappa}_\ell\|_2^2 / \|\tilde{\kappa}_\ell\|_2^2)$ evaluates the relative error between the inferred model parameter and the exact one in the simulated data, and $\exp(\mathcal{E}_{\pi_{M,t_L,C_\eta}})$ evaluates the particle diversity. Note that this optimization problem is non-convex; to ease the computational burden, we can find an approximation to C_η^* by optimizing the above objective function on a finite-size grid.

Remark 3.10. Even though we only search for the optimal hyperparameter in a finite set, the above optimization problem still requires a lot of computational resources, because for each $(\tilde{\kappa}_\ell, \tilde{x}_\ell(\cdot), \tilde{y}_\ell(\cdot))$ it needs to generate many simulated trajectories to calculate the filter. We argue that these computational resources spent on hyperparameter training are worthwhile. First, the optimal hyperparameter can make the filter more accurate than that using a random C_η . Second, the training is performed off-line, so it will not increase the computational burden of the RPF when solving a filtering problem online.

4. Numerical examples. In this section, we illustrate our approach using several numerical examples on different scales and show that the proposed regularized particle filter can significantly outperform the SIR counterpart. The code applied to perform the analy-

sis is available on GitHub: “<https://github.com/ZhouFang92/Regularized-particle-filter-for-stochastic-reaction-networks>”.

4.1. Antithetic integral feedback controller. The antithetic integral feedback (AIF) controller is a biological module that can achieve robust perfect adaptation for output species in arbitrary noisy bimolecular networks (see [4, 7]). In this example, we consider such a gene circuit (see Figure 1(a)) that has six reactions (see Figure 1(b)) and four species: the control input species (denoted by S_1), the sensing species (S_2), the regulated species (S_3), and the report species (S_4). Here, the dynamics are assumed to follow mass-action kinetics. The first three reactions in Figure 1(b) result in an “integral controller” where the integrator is $\mathbb{E}[X_1(t) - X_2(t)]$ and ensures that the mean copy number of S_3 at the stationary distribution (if it exists) is k_1/k_2 regardless of any other parameters [7]. In an *E. coli* cell, such a network can be realized by choosing the sigma factor and anti-sigma factor as S_1 and S_2 , respectively [4]. Here, we consider a filtering problem for this system in which S_4 is a fluorescent reporter and measured under a microscope, and our goal is to infer the dynamics of the regulated species (S_3) and its set point k_1/k_2 .

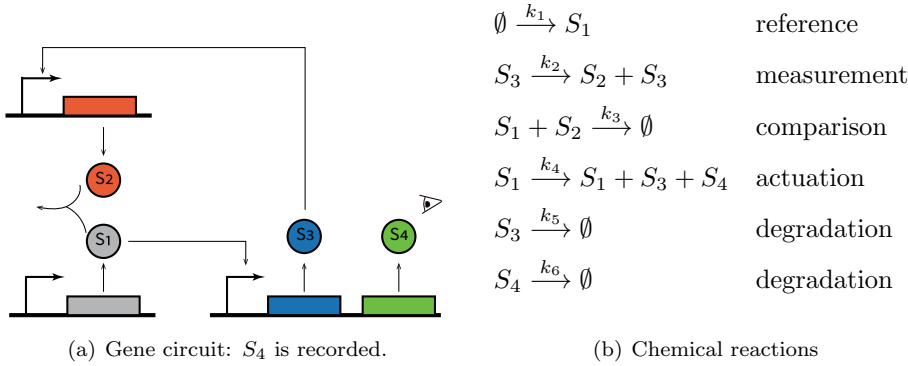


FIG. 1. **Antithetic integral feedback controller.** (a) The diagram of an antithetic integral feedback controller where S_1 and S_2 form an integral controller with the integrator $\mathbb{E}[X_1(t) - X_2(t)]$ ensuring the mean copy number of S_3 to be constant at the stationary distribution. S_4 is the report species that is visible and measured by a microscope. (b) The chemical reactions contained in the antithetic integral feedback controller. Its dynamics is assumed to follow mass-action kinetics with reaction constants k_i ($i = 1, \dots, 6$). With these parameters, the set point of the regulated species S_3 is k_1/k_2 .

Model parameter (min^{-1})	Exponent	Rescaled parameter (min^{-1})	Initial condition
$k_1 \sim \mathcal{U}(0.1, 1)$	$\beta_1 = 0$	$k'_1 \sim \mathcal{U}(0.1, 1)$	$X_1^N(0) \sim \mathcal{UI}(0, 10)$
$k_2 \sim \mathcal{U}(0.1, 1)$	$\beta_2 = 0$	$k'_2 \sim \mathcal{U}(0.1, 1)$	$X_2^N(0) \sim \mathcal{UI}(0, 10)$
$k_3 = 0.2$	$\beta_3 = 0$	$k'_3 = 0.2$	$X_3^N(0) \sim \mathcal{UI}(0, 20)$
$k_4 = 0.5$	$\beta_4 = 0$	$k'_4 = 0.5$	$X_4^N(0) \sim \mathcal{UI}(0, 20)$
$k_5 = 0.7$	$\beta_5 = 0$	$k'_5 = 0.7$	
$k_6 = 0.3$	$\beta_6 = 0$	$k'_6 = 0.3$	

TABLE 1

Model parameters of the AIF controller. \mathcal{U} is the uniform distribution, and \mathcal{UI} is the integer uniform distribution.

In this example, we set the scaling factor (N) to be 100 and the abundance coefficients ($\alpha_1, \alpha_2, \alpha_3$, and α_4) to be zero, meaning that the cell system has very few copies of the

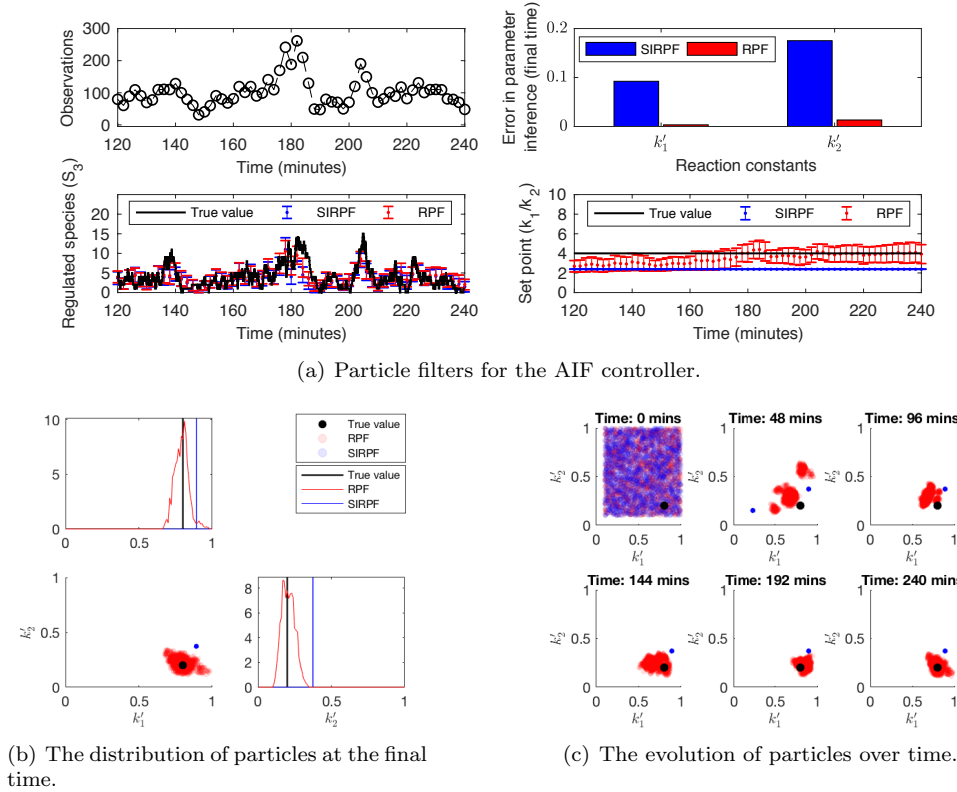


FIG. 2. **Numerical results of the AIF controller.** “RPF” stands for the regularized particle filter, and “SIRPF” stands for the sequential importance resampling particle filter. Panel (a) shows the performance of both filters in estimating the regulated species S_3 and its set point k_1/k_2 . It tells that both filters can infer the dynamics of S_3 accurately, but the RPF has a much better performance in estimating the set point and model parameters. Panel (b) presents the final time distribution of the particles associated with these filters in the parameter coordinate, and panel (c) shows the evolution of these particles over time. These two panels tell that sample degeneracy happens to the SIRPF very early in time (around 48 minutes), and, therefore, the SIRPF cannot adjust its estimate of model parameters according to the new observations afterward. This is the reason why the SIRPF fails to infer model parameters accurately. In contrast, the particle diversity in the RPF is always large, and this enables the RPF to constantly refine its estimate of model parameters according to new observations. Consequently, the RPF can infer model parameters and the set point accurately.

C_η	0	0.2	0.4	0.6	0.8	1.0	1.2	1.4	1.6	1.8*	2
Score	1.00	0.14	0.11	0.11	0.11	0.10	0.09	0.09	0.10	0.08*	0.09

TABLE 2
The performance of different C_η (the AIF controller): $t_L = 240$ (mins).

involved species. Also, we assume the model parameters to satisfy Table 1, where all the rate constants are known except for k_1 and k_2 . The observations are collected every 2 minutes and satisfy

$$Y^{\gamma_1}(t_i) = 10X_4(t_i) \wedge 1000 + W(t_i) \quad i \in \mathbb{N}_{>0},$$

in which $t_i = 2i$, and $\{W(t_i)\}_{i \in \mathbb{N}_{>0}}$ is a sequence of mutually independent standard Gaussian random variables. In this setting, we can calculate that $\gamma_1 = 0$, and the most proper RPF would

solve this filtering problem is the one utilizing the exact simulation algorithm in the sampling step (i.e., the first filter in Definition 3.1). We set the particle population of the filter to be 2000 and trained the RPF following the rule (3.2); see Table 2 for the training result. Finally, we applied the RPF with the optimal hyperparameter to a simulated process and compared its result with the SIRPF; the numerical results are shown in Figure 2.

Figure 2(a) shows that both filters can infer the dynamics of the regulated species accurately; however, the RPF has a superior performance in estimating the model parameters and the set point thanks to the larger particle diversity of the RPF (Figure 2(b) and Figure 2(c)). Moreover, the sample degeneracy of the SIRPF occurs very early in time (Figure 2(c)), suggesting that the SIRPF fails to represent the posterior of the model parameters very quickly after the starting time. All these facts suggest that the RPF outperforms the SIRPF in this numerical example.

4.2. Gene transcription model. We then consider a gene transcription model (Figure 3) consisting of four reactions (see Figure 3(b)) and three species: the inactivated gene (denoted by S_1), the activated gene (S_2), and the transcribed RNA (S_3). Moreover, we assume that the RNA contains stem-loops recognized and bound by fluorescent reporters so that the produced RNAs can be visualized in a living cell. This model resembles the gene circuit constructed in [50] for investigating and controlling transcriptional dynamics. In this example, our goal is to infer both hidden dynamic states and model parameters from the history of the RNA signal.

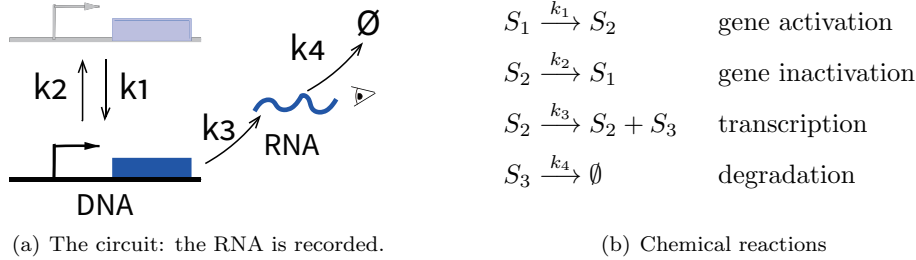


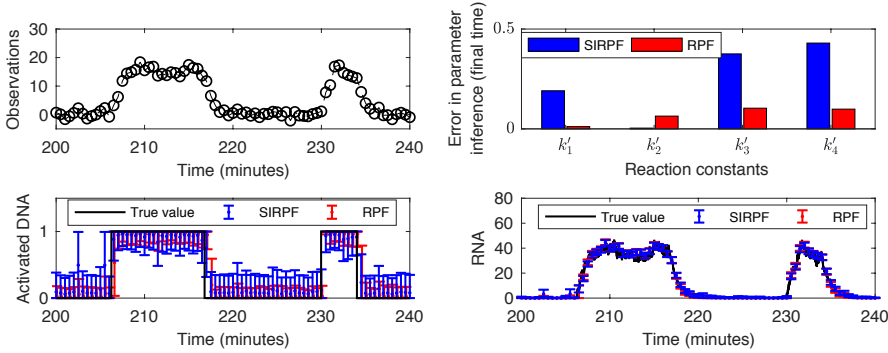
FIG. 3. **Gene transcription model.** (a) The diagram of a gene transcription circuit where the gene has “on” and “off” states and transcribes message RNAs only in the “on” state. The message RNAs are visible, and their light intensity signal is measured by a microscope. (b) The chemical reactions contained in the gene transcription model, where S_1 , S_2 , and S_3 are the inactivated gene, the activated gene, and the message RNA, respectively. All the reactions follow mass-action kinetics with reaction constants k_i ($i = 1, \dots, 4$).

Model parameter (min^{-1})	Exponent	Rescaled parameter (min^{-1})	Initial condition
$k_1 \sim \mathcal{U}(0.03, 0.3)$	$\beta_1 = 0$	$k'_1 \sim \mathcal{U}(0.03, 0.3)$	$X_1^N(0) \sim \text{Bern}(1/2)$
$k_2 \sim \mathcal{U}(0.03, 0.3)$	$\beta_2 = 0$	$k'_2 \sim \mathcal{U}(0.03, 0.3)$	$X_2^N(0) = 1 - X_1^N(0)$
$k_3 \sim \mathcal{U}(10, 100)$	$\beta_3 = 1$	$k'_3 \sim \mathcal{U}(0.2, 2)$	$X_3^N(0) \sim \frac{X_2^N(0)\text{Pois}(50)}{50}$
$k_4 \sim \mathcal{U}(0.2, 2)$	$\beta_4 = 0$	$k'_4 \sim \mathcal{U}(0.2, 2)$	

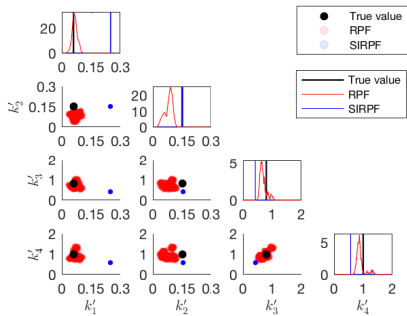
TABLE 3

Model parameters of the gene transcription model. \mathcal{U} is the uniform distribution, “Bern(·)” is the Bernoulli distribution, and “Pois” is the Poisson distribution.

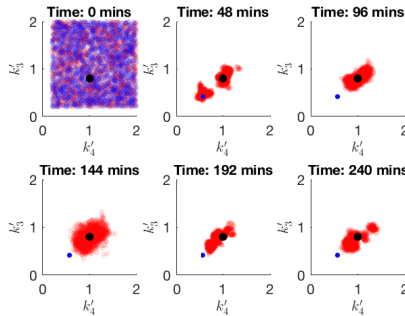
For the considered gene transcription model, we set $N = 50$, $\alpha_1 = \alpha_2 = 0$, and $\alpha_3 = 1$, meaning that the system contains very few copies of DNAs but tens of mRNA copies. Also, we assume the dynamics of the system to follow mass-action kinetics and the model parameters



(a) Particle filters for the gene transcription model.



(b) The distribution of particles at the final time.



(c) The evolution of particles over time.

FIG. 4. **Numerical results of the gene transcription model.** “RPF” stands for the regularized particle filter, and “SIRPF” stands for the sequential importance resampling particle filter. Panel (a) shows the performance of two filters in estimating the system states and model parameters. Specifically, both filters infer the dynamics of DNAs and RNAs accurately, but the RPF has a better performance in estimating model parameters. Panel (b) presents the final time distribution of the particles associated with these filters in the parameter coordinate, and panel (c) shows the time evolution of these particles. Similar to the previous example, these two panels tell that sample degeneracy happens to the SIRPF very early in time (before 48 minutes), which disables the SIRPF to adjust its estimate of model parameters according to the new observations afterward. In contrast, the RPF always has a large particle diversity and is able to refine its estimate of model parameters over time. This explains why the RPF outperforms the SIRPF in parameter inference. However, note that the RPF does not infer every parameter accurately; its estimate of k'_2 somehow deviates from the exact value (though the deviation is not too large).

C_η	0	0.1	0.2	0.3	0.4	0.5	0.6	0.7	0.8	0.9*	1
Score	1.08	0.17	0.13	0.10	0.10	0.09	0.09	0.09	0.09	0.08*	0.09

TABLE 4

The performance of different C_η (the gene transcription model): $t_L = 240$ (mins).

to satisfy Table 3 where all reaction constants are unknown. The observations are measured every 0.5 minute and satisfy

$$Y^{\gamma_1}(t_i) = 20X_3^{N, \gamma_1}(t_i) \wedge 1000 + W(t_i) \quad i \in \mathbb{N}_{>0},$$

where $\gamma_1 = 0$, $t_i = 0.5i$, 1000 is the measurement range, and $\{W(t_i)\}_{i \in \mathbb{N}_{>0}}$ is a sequence of mutually independent standard Gaussian random variables. Here, we utilized the tau-leaping

based RPF to solve the associated filtering problem. Again, we set the particle population to be 2000 and trained the filter following the rule (3.2); see Table 4 for the training results. Finally, we applied the filter to a simulated process, whose results are present in Figure 4.

Similar to the conclusion obtained in the previous subsection, Figure 4 shows that the RPF has a superior performance in estimating model parameters due to its larger particle diversity, and the sample degeneracy of the SIRPF occurs very early in time. These facts imply that RPF outperforms the SIRPF in this example. However, we note that the RPF does not infer every parameter accurately (see k'_2 in Figure 4(b)); this might be due to the fact that particle population is not large enough in this example. Also, both filters have similar performances in estimating the gene dynamics (Figure 4(a)) due to the simple structure of the system: once the observation increases/decreases sharply, the filter can learn that the gene is turned on/off whatever its estimates of model parameters.

4.3. Transcription regulation network. Finally, we consider a transcription regulation network (Figure 5) where the gene product inhibits the gene expression process by binding to the DNA molecule. This system consists of six reactions (see Figure 5(b)) and four chemical species: the inactivated gene (denoted by S_1), the activated gene (S_2), the mRNA (S_3), and the protein (S_4). Also, we assume that the protein is fluorescent and, therefore, can be measured by a microscope. In this example, our goal is to infer both the hidden dynamic states and model parameters from the time-course data.

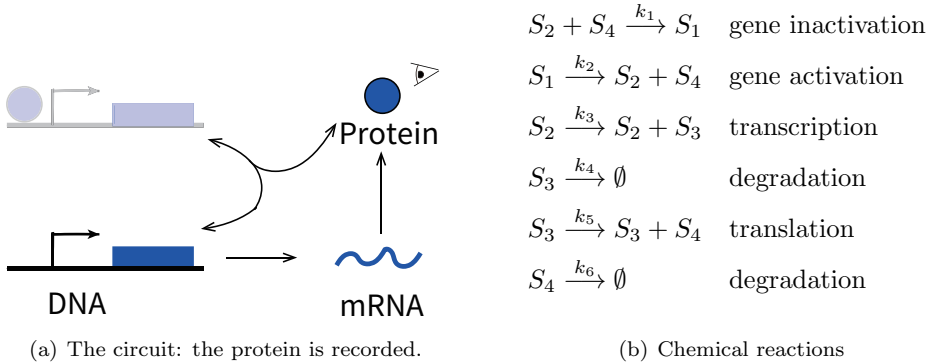


FIG. 5. **Transcription regulation network.** (a) The diagram of a transcription regulation network, where the gene product (the protein) inhibits transcription by silencing the gene. The protein contains a fluorescent tag so that it is visible and measured by a microscope. (b) The chemical reactions contained in the transcription regulation network, where S_1 , S_2 , S_3 , and S_4 are the inactivated gene, the activated gene, the mRNA, and the protein, respectively. All the reactions follow the mass-action kinetics with reaction constants k_i ($i = 1, \dots, 6$).

The modeling of the systems is as follows. We set $N = 10^4$, $\alpha_1 = \alpha_2 = \alpha_3 = 0$, and $\alpha_4 = 1$; in other words, the system has very few copies of DNA molecules and mRNA molecules but a large number of proteins. Also, we assume that the system dynamics to follow mass-action kinetics and the model parameters to satisfy Table 5. Based on it, we can easily calculate that the first timescale γ_1 equals to 0. The observations are collected every 2 minutes and satisfy

$$Y^{\gamma_1}(t_i) = 20X_4^{N, \gamma_1}(t_i) \wedge 1000 + W(t_i) \quad i \in \mathbb{N}_{>0},$$

where $t_i = 2i$, 1000 is the measurement range, and $\{W(t_i)\}_{i \in \mathbb{N}_{>0}}$ is a sequence of mutually independent standard Gaussian random variables. In this setting, the most proper filter for the considered system is the RPF using PDMPs in sampling (the third one in Definition 3.1). Again, we set the particle population to be 2000 and trained the filter following the rule (3.2);

Model parameter (min^{-1})	Exponent	Rescaled parameter (min^{-1})	Initial condition
$k_1 \sim \mathcal{U}(0.03, 0.3)$	$\beta_1 = 0$	$k'_1 \sim \mathcal{U}(0.03, 0.3)$	$X_1^N(0) \sim \text{Bern}(1/2)$
$k_2 \sim \mathcal{U}(0.03, 0.3)$	$\beta_2 = 0$	$k'_2 \sim \mathcal{U}(0.03, 0.3)$	$X_2^N(0) = 1 - X_1^N(0)$
$k_3 \sim \mathcal{U}(0.1, 1)$	$\beta_3 = 0$	$k'_3 \sim \mathcal{U}(0.1, 1)$	$X_3^N(0) \sim \text{Poiss}(10)$
$k_4 \sim \mathcal{U}(0.1, 1)$	$\beta_4 = 0$	$k'_4 \sim \mathcal{U}(0.1, 1)$	$X_4^N(0) \sim \frac{\text{Poiss}(10^4)}{10^4}$
$k_5 \sim \mathcal{U}(10^3, 10^4)$	$\beta_5 = 1$	$k'_5 \sim \mathcal{U}(0.1, 1)$	
$k_6 \sim \mathcal{U}(0.1, 1)$	$\beta_6 = 0$	$k'_6 \sim \mathcal{U}(0.1, 1)$	

TABLE 5

Model parameters of the transcription regulation model: \mathcal{U} is the uniform distribution, “Bern(\cdot)” is the Bernoulli distribution, and “Poiss” is the Poisson distribution.

C_η	0	0.2	0.4	0.6	0.8	1.0	1.2	1.4	1.6	1.8*	2
Score	1.29	0.41	0.37	0.34	0.37	0.36	0.36	0.36	0.35	0.33*	0.36

TABLE 6

The performance of different C_η (the transcription regulation network): $t_L = 240$ (mins).

see Table 6 for the training results. Finally, we applied the filter to a simulated process, whose results are present in Figure 6.

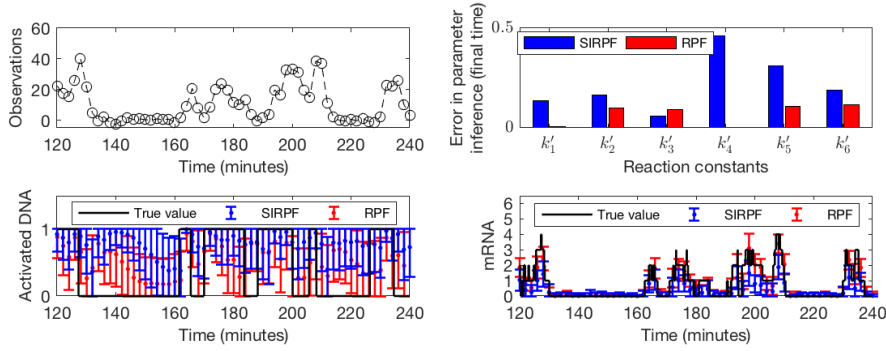
Similar to the previous examples, the RPF outperforms the SIRPF in this example in estimating model parameters and the mRNA dynamics¹ due to its large particle diversity (Figure 6). Moreover, even though the initial estimate is not very accurate, the particles in the RPF can gradually approach the exact value of the model parameters and, consequently, provide an accurate estimate of the model parameters at the final time (Figure 6(c)).

Despite these successes, we can observe that both filters fail to precisely estimate the gene state (Figure 6(a)). This is attributed to the long time delay between the gene dynamics and the protein dynamics, which makes the exact posterior of the gene state very noisy. Inspired by this observation, we argue that given an arbitrary gene circuit, it is not reasonable to expect the filter to infer every species accurately, especially those to whose changes the fluorescent reporters respond slowly.

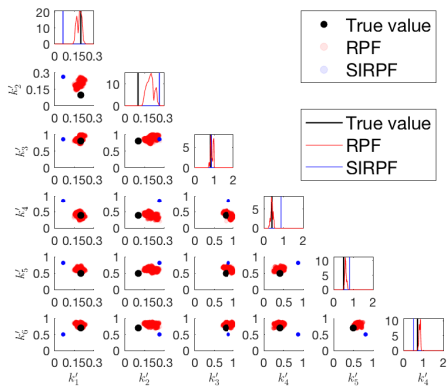
5. Conclusion. The simultaneous inference of hidden dynamic states and model parameters of a stochastic reaction network is an important and difficult task. One challenge lies in the high computational complexity of the exact simulation method for the stochastic reaction dynamics, which makes the particle filter, a simulation-based algorithm, computationally inefficient. Moreover, the sample degeneracy occurring in conventional particle filters has a negative impact on the accuracy of the estimate. To tackle these problems, this paper introduced regularized particle filters (RPFs) for stochastic reaction networks (SRNs) on different scales using computationally efficient simulation algorithms. Specifically, the filter chooses the proper simulation algorithm for sampling based on the scale of the system considered so that the computational time is acceptable (Subsection 2.4.3 and Definition 3.1). Also, an artificial evolution step is executed after resampling to mitigate sample degeneracy and cope with the fluctuation of model parameters in practical systems (Remark 3.3). Furthermore, by parameter sensitivity analyses, we showed that the constructed RPF is convergent to the exact filter for a broad class of SRNs (Theorem 3.8 and Remark 3.9). Finally, several numerical examples were shown to illustrate the superior performance of the constructed RPF compared with its sequential-importance-resampling (SIR) counterpart.

From the numerical examples, we can observe that the constructed RPF also has some

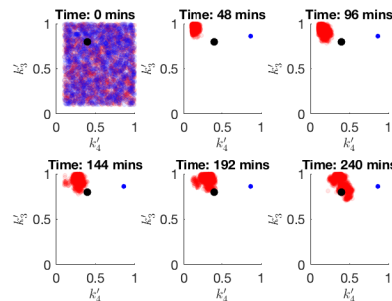
¹The SIRPF underestimates the mRNA dynamics for many times; see the result around 200 minutes.



(a) Particle filters for the gene transcription model.



(b) The distribution of particles at the final time.



(c) The evolution of particles over time.

FIG. 6. **Numerical results of the gene transcription model.** “RPF” stands for the regularized particle filter, and “SIRPF” stands for the sequential importance resampling particle filter. Panel (a) shows the performance of both filters in estimating the hidden system states and model parameters. Specifically, RPF has a superior performance in estimating the dynamics of mRNAs and model parameters. (Note that the SIRPF underestimates the mRNA dynamics many times around 200 minutes.) However, both filters fail to infer the DNA states accurately. Panel (b) shows the final time distribution of the particles associated with these filters in the parameter coordinate, and panel (c) shows the time evolution of these particles. Similar to the previous examples, these two panels tell that sample degeneracy happens to the SIRPF very early in time (before 48 minutes), which disables the SIRPF to adjust its estimate of model parameters according to the new observations afterward. In contrast, the RPF always has a large particle diversity and is able to refine its estimate of model parameters to approach the exact value. This is the reason why the RPF outperforms the SIRPF in estimating model parameters. Also, note that the RPF does not infer every parameter very accurately; its estimate of k'_2 (the reaction constant for gene activation) somehow deviates from the exact value.

drawbacks; for instance, not every parameter can be inferred accurately when the number of unknown parameters is large. This suggests that the filter does not scale very well with the system dimension. A possible solution to this problem is the Rao-Blackwellization method [43], in which some variables are marginalized out so that the filter only needs to simulate a model of reduced dimensionality. For mass-action networks, such a scalable filter has been provided in [60], where the model parameters are integrated out by assuming their priors to be Gamma distributions. However, the theory for general kinetics is still undeveloped, and the combination of it with the RPF also remains to be investigated. Furthermore, the

numerical examples indicate that the posterior of some hidden dynamic variables can be either very noisy or extremely narrow disregarding the model parameters (see the discussion in [Subsection 4.2](#) and [Subsection 4.3](#)). This means that these variables are either impossible to infer accurately or can be learned in a more clever way with biological insights into the system. Consequently, eliminating these variables can be another option to further reduce the system and improve the filter. Lastly, it is known that unweighted particle filters can avoid the curse of dimensionality in some circumstances [55]; therefore, it is worth applying this methodology to biological filtering problems. However, conventional unweighted particle filters (e.g., the particle flow method [12] and feedback particle filters [59]) are designed for systems of continuous state spaces. For SRNs whose state space is discrete, one needs to significantly modify the theory and algorithms.

Appendix A. The proof of [Theorem 3.8](#).

We first outline the strategy to prove our main result. Note that the error of a particle filter comes from model reduction, finite sampling, resampling, and artificial evolution. Here, we can easily analyze the error introduced by model reduction using the convergence of reduced models and investigate the error caused by finite sampling and resampling using the tools in [13, 9, 5]. Therefore, the key to proving our main result lies in the analysis of artificial evolution. In this appendix, we show that the error caused by artificial evolution is of the order $\frac{1}{\sqrt{M}}$ (where M is the particle population) by the parameter sensitivity analysis, and, thus, this error vanishes as the particle population goes to infinity. Finally, by combining all the error analysis results, we can prove the main theorem.

To make the idea more explicit, we formulate the proof outline as follows. First, since the model reduction is not the key factor in this proof, we simplify the notation by removing the superscript that specifies the dynamical model applied. Specifically, for a given RPF constructed in [Definition 3.1](#), we term

$$\begin{aligned}
 \bar{\pi}_{M,t_i}(\phi) & \text{ as the particle filter } \bar{\pi}_{M,t_i}^{N,\gamma_1}(\phi), \bar{\pi}_{M,t_i}^{N,\gamma_1,\tau}(\phi), \text{ or } \bar{\pi}_{M,t_i}^{N,\gamma_1,H}(\phi), \\
 \hat{\pi}_{M,t_i}(\phi) & \text{ as the estimate of the function } \phi \text{ based on resampled particles} \\
 & \quad (\hat{\pi}_{M,t_i}(\phi) \triangleq \frac{1}{M} \sum_{j=1}^M \phi(\hat{\kappa}_j(t_i), \bar{x}_j(t_i))), \\
 \tilde{\pi}_{M,t_i}(\phi) & \text{ as the estimate of the function } \phi \text{ based on artificially perturbed} \\
 & \quad \text{particles } (\tilde{\pi}_{M,t_i}(\phi) \triangleq \frac{1}{M} \sum_{j=1}^M \phi(\bar{\kappa}_j(t_i), \bar{x}_j(t_i))), \\
 \pi_{t_{i+1}}(\phi) & \text{ as the exact filter } \pi_{t_{i+1}}^{N,\gamma_1}(\phi), \\
 K_t & \text{ as the transition kernel of the applied dynamical system} \\
 & \quad \text{(the CTMC, tau-leaping model, or PDMP),} \\
 K_t^{N,\gamma_1} & \text{ as the transition kernel of the full model} \\
 Y(t_i) & \text{ as the observation } Y^{N,\gamma_1}(t_i), \\
 \Delta t_i & \text{ as } t_{i+1} - t_i.
 \end{aligned}
 \tag{A.1}$$

With these notations, we can decompose the error between the RPF $\bar{\pi}_{M,t_{i+1}}(\phi)$ and the

exact filter $\pi_{t_{i+1}}(\phi)$ as follows.

$$\begin{aligned}
\bar{\pi}_{M,t_{i+1}}(\phi) - \pi_{t_{i+1}}(\phi) &= \bar{\pi}_{M,t_{i+1}}(\phi) - \frac{\pi_{t_i}(K_{\Delta t_i}^{N,\gamma_1} \ell_{Y(t_{i+1})} \phi)}{\pi_{t_i}(K_{\Delta t_i}^{N,\gamma_1} \ell_{Y(t_{i+1})})} \\
\text{(A.2)} \quad &= \underbrace{\left(\bar{\pi}_{M,t_{i+1}}(\phi) - \frac{\tilde{\pi}_{M,t_i}(K_{\Delta t_i} \ell_{Y(t_{i+1})} \phi)}{Z_t} \right)}_{\text{the error caused by finite sampling}} \\
&\quad + \frac{1}{Z_t} \underbrace{\left(\tilde{\pi}_{M,t_i}(K_{\Delta t_i} \ell_{Y(t_{i+1})} \phi) - \hat{\pi}_{M,t_i}(K_{\Delta t_i} \ell_{Y(t_{i+1})} \phi) \right)}_{\text{the error caused by the artificial evolution}} \\
&\quad + \frac{1}{Z_t} \underbrace{\left(\hat{\pi}_{M,t_i}(K_{\Delta t_i} \ell_{Y(t_{i+1})} \phi) - \bar{\pi}_{M,t_i}(K_{\Delta t_i} \ell_{Y(t_{i+1})} \phi) \right)}_{\text{the error caused by resampling}} \\
&\quad + \frac{1}{Z_t} \underbrace{\left(\bar{\pi}_{M,t_i}(K_{\Delta t_i} \ell_{Y(t_{i+1})} \phi) - \bar{\pi}_{M,t_i}(K_{\Delta t_i}^{N,\gamma_1} \ell_{Y(t_{i+1})} \phi) \right)}_{\text{the error caused by model reduction}} \\
&\quad + \frac{1}{Z_t} \underbrace{\left(\bar{\pi}_{M,t_i}(K_{\Delta t_i}^{N,\gamma_1} \ell_{Y(t_{i+1})} \phi) - \pi_{t_i}(K_{\Delta t_i}^{N,\gamma_1} \ell_{Y(t_{i+1})} \phi) \right)}_{\text{the error of the particle filter at } t_i}
\end{aligned}$$

where the first equality follows from the recursive formulas (2.2) and (2.3), the term $\ell_{Y(t_{i+1})}$ is the likelihood function (see (2.3) and the text below), and $Z_t = \pi_{t_i}(K_{\Delta t_i}^{N,\gamma_1} \ell_{Y(t_{i+1})})$. We note that for given observations, both the likelihood function and Z_t are lower bounded by a positive constant due to the boundedness of $h(\cdot)$ (see subsection 2.3), so $\frac{1}{Z_t}$ is uniformly upper bounded and, therefore, not a concern in the error analysis. (A.2) tells that the error analysis of a particle filter can be performed in a recursive fashion where one analyzes the error of the filter at time t_{i+1} after estimating the error at time t_i . Therefore, the key to proving our result lies in investigating the first four terms on the right hand side of this equality, which corresponds to finite sampling, artificial evolution, resampling, and model reduction, respectively. We also note that the first and the third terms have already been analyzed in the classical literature [13, 9, 5], and the fourth can be analyzed by the convergence of the reduced model. Consequently, the most challenging part is to analyze the second term, which corresponds to the error caused by the artificial evolution step.

Technically, we estimate the second moment of the error caused by artificial evolution. Notice that for any function ϕ satisfying (3.1), we can find a positive constant \tilde{C}_ϕ such that

$$\begin{aligned}
\text{(A.3)} \quad &\mathbb{E} \left[\left| \bar{\pi}_{M,t_{i+1}}(\phi) - \hat{\pi}_{M,t_{i+1}}(\phi) \right|^2 \middle| \mathcal{Y}_{t_{i+1}} \right] \\
&= \mathbb{E} \left[\left| \frac{1}{M} \sum_{j=1}^M \phi(\hat{\kappa}_j(t_{i+1}), \bar{x}_j(t_{i+1})) - \phi(\bar{\kappa}_j(t_{i+1}), \bar{x}_j(t_{i+1})) \right|^2 \middle| \mathcal{Y}_{t_{i+1}} \right] \\
&\leq \frac{\tilde{C}_\phi^2}{M} \sum_{j=1}^M \mathbb{E} \left[\|\bar{\kappa}_j(t_{i+1}) - \hat{\kappa}_j(t_{i+1})\|_2^2 (1 + \|\bar{x}_j(t_{i+1})\|_2^q)^2 \middle| \mathcal{Y}_{t_{i+1}} \right] \\
&\leq \frac{\tilde{C}_\phi^2 C_\eta^2 \mathcal{V}}{M} \sum_{j=1}^M \frac{1}{M} \mathbb{E} \left[(1 + \|\bar{x}_j(t_{i+1})\|_2^q)^2 \middle| \mathcal{Y}_{t_{i+1}} \right]
\end{aligned}$$

where the third line follows from the midpoint theorem and the Jensen inequality, and the last line follows from Assumption 3.2. Therefore, we can analyze the effect of artificial evolution by checking whether $K_{\Delta t_i} \ell_{Y(t_{i+1})} \phi$ satisfies (3.1) and estimating the conditional moments of particles $\sum_{j=1}^M \frac{1}{M} \mathbb{E} \left[(1 + \|\bar{x}_j(t_{i+1})\|_2^q)^2 \middle| \mathcal{Y}_{t_{i+1}} \right]$, of which the former corresponds to the parameter sensitivity analysis of the transition kernel.

Following this idea, in [Appendix A.1](#), we use the parameter sensitivity analysis to show that the second term on the right hand side of [\(A.2\)](#) is of order $\frac{1}{\sqrt{M}}$. Specifically, we first prove in [Appendix A.1](#) that both the state vector and the parameter sensitivity for the transition kernel grow mildly under the assumed conditions ([Proposition A.1](#) and [Proposition A.2](#)). Then, based on these results and [\(A.3\)](#), we can find a $\mathcal{Y}_{t_{i+1}}$ measurable random variable $\tilde{C}_{t_{i+1}}$ such that

$$\mathbb{E} \left[\left| \text{the second term on the right hand side of (A.2)} \right|^2 \middle| \mathcal{Y}_{t_{i+1}} \right] \leq \frac{\tilde{C}_{t_{i+1}}}{M},$$

which indicates that the error caused by artificial evolution is of order $\frac{1}{\sqrt{M}}$ (see [Remark A.3](#)). Finally, based on the obtained results, we prove the convergence of the established RPF by mathematical induction in [Appendix A.2](#).

A.1. Parameter sensitivities for transition kernels and the analysis of the error introduced by artificial evolution. In this subsection, we use the parameter sensitivity analysis to estimate the error introduced by the artificial evolution and show that it vanishes as the particle population goes to infinity. Recall that the key is to show $K_{\Delta t_i} \ell_{\mathcal{Y}(t_{i+1})} \phi$ satisfying [\(3.1\)](#) and moments of particles being bounded from above (see [\(A.3\)](#)).

First, [Assumption 3.6](#) and [Assumption 2.1](#) suggest that any moment of the state vector is bounded, and, therefore, the moments of particles are also bounded.

PROPOSITION A.1 (Adapted from [\[27, Lemma 5.1\]](#) and [\[45, Theorem 4.5\]](#)). *If [Assumption 3.6](#) holds, then for all $p > 0$, there exists a positive constant C_p such that*

$$\begin{aligned} \mathbb{E} \left[\left\| X^{N, \gamma_1}(t) \right\|_2^p \middle| \mathcal{K} = \kappa, X^{N, \gamma_1}(0) = x \right] &\leq (\|x\|_2^p + C_p t) e^{C_p t} \\ \mathbb{E} \left[\|X^{\gamma_1}(t)\|_2^p \middle| \mathcal{K} = \kappa, X^{\gamma_1}(0) = x \right] &\leq (\|x\|_2^p + C_p t) e^{C_p t} \end{aligned}$$

for any $t > 0$ and $(\kappa, x) \in \Theta \times \mathbb{R}_{\geq 0}^n$. If moreover [Assumption 2.1](#) holds, then for $p > 0$, there exists a constant $C_{p, \tau}$ such that

$$\sup_{t \in [0, T]} \mathbb{E} \left[\left\| X_\tau^{N, \gamma_1}(t) \right\|_2^p \middle| \mathcal{K} = \kappa, X_\tau^{N, \gamma_1}(t) = x \right] \leq (\|x\|_2^p + 1) e^{C_{p, \tau} t}$$

for all $(\kappa, x) \in \Theta \times \mathbb{R}_{\geq 0}^n$.

Proof. The results for the full model and the PDMP are adapted from [\[27, Lemma 5.1\]](#); the result for the tau-leaping method is adapted from [\[45, Theorem 4.5\]](#). \square

Then, we look at the parameter sensitivity for the CTMC, tau-leaping model, and PDMP. Given an initial condition (κ, x) and a time point t , we term

$$\begin{aligned} \Psi_{t, g}^N(\kappa, x) &= \mathbb{E} \left[g \left(X^{N, \gamma_1}(t) \right) \middle| \mathcal{K} \triangleq \kappa, X^{N, \gamma_1}(0) = x \right], \\ \Psi_{t, g}^{N, \tau}(\kappa, x) &= \mathbb{E} \left[g \left(X_\tau^{N, \gamma_1}(t) \right) \middle| \mathcal{K} \triangleq \kappa, X^N(0) = x \right], \\ \Psi_{t, g}(\kappa, x) &= \mathbb{E} \left[g \left(X^{\gamma_1}(t) \right) \middle| \mathcal{K} \triangleq \kappa, X^{N, \gamma_1}(0) = x \right] \end{aligned}$$

as the conditional expectations of function g for the CTMC, tau-leaping model, and PDMP, respectively. Then, the parameter sensitivity for these models are defined, respectively, by $\frac{\partial \Psi_{t, g}^N(\kappa, x)}{\partial \kappa}$, $\frac{\partial \Psi_{t, g}^{N, \tau}(\kappa, x)}{\partial \kappa}$, and $\frac{\partial \Psi_{t, g}(\kappa, x)}{\partial \kappa}$. The literature [\[29\]](#) shows that the parameter sensitivity for the full model can be computed by

$$\begin{aligned} \text{(A.4)} \quad &\frac{\partial \Psi_{t, g}^N(\kappa, x)}{\partial \kappa} \\ &= \sum_{j=1}^r \mathbb{E} \left[\int_0^t \frac{\partial \lambda_j^N(\kappa, X^{N, \gamma_1}(s))}{\partial \kappa} \Delta_j^N \Psi_{t-s, g}^N(\kappa, X^{N, \gamma_1}(s)) \, ds \middle| \mathcal{K} = \kappa, X^N(0) = x \right] \end{aligned}$$

where $\Delta_j^N \Psi_{t-s,g}^N(\kappa, x) \triangleq \Psi_{t-s,g}^N(\kappa, x + \Lambda^N \zeta_j) - \Psi_{t-s,g}^N(\kappa, x)$. Similarly, by mathematical induction, we can show that the parameter sensitivity for the tau-leaping model (with a deterministic time-discretization scheme) can be computed by ²

$$(A.5) \quad \frac{\partial \Psi_{t,g}^{N,\tau}(\kappa, x)}{\partial \kappa} = \sum_{j=1}^r \mathbb{E} \left[\sum_{\tau_i < t} (\tau_{i+1} \wedge t - \tau_i) \frac{\partial \lambda_j^N(\kappa, X_\tau^{N,\gamma_1}(\tau_i))}{\partial \kappa} \Delta_j^N \Psi_{t-s,g}^N(\kappa, X_\tau^{N,\gamma_1}(\tau_{i+1})) \right. \\ \left. \Big| \mathcal{K} = \kappa, X_\tau^{N,\gamma_1}(0) = x \right].$$

Finally, the literature [28] tells that under [Assumption 2.3](#), [Assumption 3.6](#), and [Assumption 3.7](#), the parameter sensitivity for the PDMP satisfies

$$(A.6) \quad \frac{\partial \Psi_{t,g}(\kappa, x)}{\partial \kappa} = \lim_{N \rightarrow \infty} \frac{\partial \Psi_{t,g}^N(\kappa, x)}{\partial \kappa},$$

if g is bounded, continuously differentiable. Using these results, we can further prove that the parameter sensitivity for the transition kernel is at most polynomially growing with respect to the state argument (see [Proposition A.2](#)).

PROPOSITION A.2. (*Polynomially growing rate of the parameter sensitivity for the transition kernel*) For any measurable function ϕ , we denote

$$\begin{aligned} (K_t^{N,\gamma_1} \phi)(\kappa, x) &\triangleq \mathbb{E}_{\mathbb{P}} \left[\phi \left(\mathcal{K}, X^{N,\gamma_1}(t) \right) \Big| \mathcal{K} = \kappa, X^N(0) = x \right], \\ (K_t^{N,\gamma_1,\tau} \phi)(\kappa, x) &\triangleq \mathbb{E}_{\mathbb{P}} \left[\phi \left(\mathcal{K}, X_\tau^{N,\gamma_1}(t) \right) \Big| \mathcal{K} = \kappa, X^N(0) = x \right], \\ (K_t^{\gamma_1} \phi)(\kappa, x) &\triangleq \mathbb{E}_{\mathbb{P}} [\phi(\mathcal{K}, X^{\gamma_1}(t)) \mid \mathcal{K} = \kappa, X^{\gamma_1}(0) = x]. \end{aligned}$$

If $\phi : \Theta \times \mathbb{R}_{\geq 0}^n \rightarrow \mathbb{R}$ satisfies the requirement in [Theorem 3.8](#), then the following results hold.

- If [Assumption 3.6](#) holds, then for any $t > 0$ there exists a constant $C_{t,\phi}$ such that $\left\| \frac{\partial (K_t^{N,\gamma_1} \phi)(\kappa, x)}{\partial \kappa} \right\|_2 \leq C_{t,\phi} (1 + \|x\|_2^q)$ for all $(\kappa, x) \in \Theta \times \mathbb{R}_{\geq 0}^n$.
- If [Assumption 2.1](#) and [Assumption 3.6](#) hold, then for any $t > 0$ there exists a constant $C_{t,\phi,\tau}$ such that $\left\| \frac{\partial (K_t^{N,\gamma_1,\tau} \phi)(\kappa, x)}{\partial \kappa} \right\|_2 \leq C_{t,\phi,\tau} (1 + \|x\|_2^q)$ for all $(\kappa, x) \in \Theta \times \mathbb{R}_{\geq 0}^n$.
- If [Assumption 2.3](#), [Assumption 3.6](#), and [Assumption 3.7](#) hold, then for any $t > 0$ and $(\kappa, x) \in \Theta \times \mathbb{R}_{\geq 0}^n$ there holds $\left\| \frac{\partial (K_t^{\gamma_1} \phi)(\kappa, x)}{\partial \kappa} \right\|_2 \leq C_{t,\phi} (1 + \|x\|_2^q)$, where $C_{t,\phi}$ is the same as that in the first result.

Proof. We first prove the result for the transition kernel of the full model. By definition, we can write the derivative of the transition kernel by

$$\frac{\partial K_t^{N,\gamma_1} \phi(\kappa, x)}{\partial \kappa} = \mathbb{E} \left[\frac{\partial \phi(\kappa, X^{N,\gamma_1}(t))}{\partial \kappa} \Big| \mathcal{K} = \kappa, X^{\gamma_1}(0) = x \right] + \frac{\partial \Psi_{t,\phi(\kappa,\cdot)}^N(\theta, x)}{\partial \theta} \Big|_{\theta=\kappa}.$$

By (3.1) and [Proposition A.1](#), we can find a positive constant $C_{t,\phi}^1$ such that

$$(A.7) \quad \mathbb{E} \left[\left\| \frac{\partial \phi(\kappa, X^{N,\gamma_1}(t))}{\partial \kappa} \right\|_2 \Big| \mathcal{K} = \kappa, X^{\gamma_1}(0) = x \right] \leq C_{t,\phi}^1 (1 + \|x\|_2^q)$$

²Note that $\frac{\partial \Psi_{t,g}^{N,\tau}(\kappa, x)}{\partial \kappa}$ computes the parameter sensitivity when the tau-leaping model is viewed as the ground truth. It is not necessarily equal or even close to $\frac{\partial \Psi_{t,g}^N(\kappa, x)}{\partial \kappa}$, the parameter sensitivity for the full model.

for all $(\kappa, x) \in \Theta \times \mathbb{R}_{\geq 0}^n$. Also, by (A.4) and the boundedness of ϕ , there holds

$$\begin{aligned} \left\| \frac{\partial \Psi_{t, \phi(\kappa, \cdot)}^N(\theta, x)}{\partial \theta} \Big|_{\theta = \kappa} \right\|_2 &\leq 2\|\phi\|_\infty \sum_{j=1}^r \left\| \mathbb{E} \left[\int_0^t \frac{\partial \lambda_j^N(\kappa, X^{N, \gamma_1}(s))}{\partial \kappa} ds \Big| \mathcal{K} = \kappa, X^N(0) = x \right] \right\|_2 \\ &\leq 2\|\phi\|_\infty \sum_{j=1}^r \mathbb{E} \left[\int_0^t \left\| \frac{\partial \lambda_j^N(\kappa, X^{N, \gamma_1}(s))}{\partial \kappa} \right\|_2 ds \Big| \mathcal{K} = \kappa, X^N(0) = x \right] \end{aligned}$$

where the second inequality follows from Jensen's inequality and the triangle inequality. Therefore by Proposition A.1 and Assumption 3.6, we can find a constant $C_{t, \phi}^2$ such that

$$(A.8) \quad \left\| \frac{\partial \Psi_{t, \phi(\kappa, \cdot)}^N(\theta, x)}{\partial \theta} \Big|_{\theta = \kappa} \right\|_2 \leq C_{t, \phi}^2 (1 + \|x\|_2^q) \quad \forall (\kappa, x) \in \Theta \times \mathbb{R}_{\geq 0}^n.$$

Finally, by combing (A.7) and (A.8), we prove the result for the transition kernel of the full model (the first result).

By the same argument, we can also prove the second result. For the third result, we can learn from (A.6) that $\Psi_{t, \phi(\kappa, \cdot)}(\theta, x)$ satisfies (A.8). Moreover, by (3.1) and Proposition A.1, we can show that the quantity $\phi(\kappa, X^{\gamma_1}(t))$ also satisfies (A.7). Therefore, the third result is proven. \square

Remark A.3 (Analysis of the error introduced by artificial evolution). Now, we use the obtained propositions to show that the second term on the right hand side of (A.2) is of the order $1/\sqrt{M}$. First, we look at the conditional moments of the particles in the RPF. We note that every weight $w_j(t_i)$ ($j = 1, \dots, M$, $i = 1, 2, \dots$) is upper bounded by the constant $\frac{1}{M} \exp(\|Y(t_i)\|_2^2 + m\|h\|_\infty^2)$, and the resampling does not change the expectation of the empirical mean of these weighted particles. These facts together with the third claim of Assumption 3.6 and Proposition A.1 suggests that given the observation process, the second conditional moment of the particles is bounded from above, i.e.,

$$(A.9) \quad \frac{1}{M} \sum_{j=1}^n \mathbb{E} \left[(1 + \|\bar{x}_j(t_{i+1})\|_2^q)^2 | \mathcal{Y}_{t_{i+1}} \right] \leq \tilde{C}_{Y(t_{i+1})}$$

where $\tilde{C}_{Y(t_{i+1})}$ is a $\mathcal{Y}_{t_{i+1}}$ measurable random variable. Second, we note that if ϕ satisfies the requirement in Theorem 3.8, the function $\ell_y \phi$ (for any $y \in \mathbb{R}^m$) also satisfies this requirement, because the likelihood function ℓ_y is bounded and has no dependence on the argument κ . Consequently, by Proposition A.2, the function $K_{\Delta t_i} \ell_{Y(t_{i+1})} \phi$ also satisfies the requirement in Theorem 3.8 under the proposed conditions. Finally, applying these results to (A.3), we can find a $\mathcal{Y}_{t_{i+1}}$ measurable random variable $\tilde{C}_{t_{i+1}}$ such that

$$(A.10) \quad \mathbb{E} \left[\left| \text{the 2nd term on the right hand side of (A.2)} \right|^2 | \mathcal{Y}_{t_{i+1}} \right] \leq \frac{\tilde{C}_{t_{i+1}}}{M},$$

which suggests that the bias contributed by artificial evolution is of order $\frac{1}{\sqrt{M}}$.

A.2. Proving the main result by mathematical induction. In this subsection, we prove Theorem 3.8 using the results obtained in the previous section.

The Proof of Theorem 3.8. For simplicity, we use the simplified notations in (A.1) to prove the result. Moreover, we introduce another quantity a to indicate the fidelity of the reduced model. Specifically, if the RPF uses the tau-leaping model, then $a = |\tau|$; if the RPF uses the PDMP model, then $a = 1/N$; if the RPF uses the full model, then $a \equiv 0$. By the dominated convergence theorem, to prove the result, we only need to show

$$(A.11) \quad \lim_{M \rightarrow \infty} \lim_{a \rightarrow \infty} \mathbb{E} \left[(\bar{\pi}_{M, t_i}(\phi) - \pi_{t_i}(\phi))^2 | \mathcal{Y}_{t_i} \right] = 0$$

for any $i \in \mathbb{N}_{\geq 0}$ and any ϕ satisfying the requirement in [Theorem 3.8](#). Therefore, in the sequel, we focus on analyzing the conditional error of the filters.

We use mathematical induction to prove [\(A.11\)](#). For $i = 1$, the relation [\(A.11\)](#) holds automatically by the law of large numbers and the convergence of the reduced models. Then, we are going to show that if [\(A.11\)](#) holds for a positive integer i , then it also holds for the positive integer $i + 1$. Note that we can decompose the error of the filter as [\(A.2\)](#); therefore, the key is to separately analyze the error caused by finite sampling, artificial evolution, resampling, and model reduction.

Error caused by model reduction: Recall that for given observations, both the likelihood function and Z_t in [\(A.2\)](#) are lower bounded by a positive constant due to the boundedness of $h(\cdot)$ (see [subsection 2.3](#)), so $\frac{1}{Z_i}$ is uniformly upper bounded and, therefore, not a concern in the error analysis. Then, by the convergence of the reduced models ([Assumption 2.2](#) and [Proposition 2.4](#)) and the conditional dominated convergence theorem, we have that for any bounded continuous function ϕ , there holds

$$(A.12) \quad \lim_{a \rightarrow 0} \mathbb{E} \left[(\text{the 4th term on the RHS of (A.2)})^2 \middle| \mathcal{Y}_{t_{i+1}} \right] = 0.$$

Error caused by resampling: If we use the multinomial resampling, then all the resampled particles are conditionally independently and identically distributed given the observation process, and, therefore, we can conclude [\[9\]](#)

$$\mathbb{E} \left[\left| \hat{\pi}_{M,t_i} (K_{\Delta t_i} \ell_{Y(t_{i+1})} \phi) - \bar{\pi}_{M,t_{i+1}} (K_{\Delta t_i} \ell_{Y(t_{i+1})} \phi) \right|^2 \middle| \mathcal{Y}_{t_{i+1}} \right] \leq \frac{\|\ell_{Y(t_{i+1})} \phi\|_\infty^2}{M},$$

where $\|\ell_{Y(t_{i+1})} \phi\|_\infty$ is the uniform norm of the function $\ell_{Y(t_{i+1})} \phi$. Moreover, by [\[5, Exercise 9.1\]](#) which states that residual resampling introduces the minimum noise among all resampling methods, we can also conclude the above relation for residual resampling, and, therefore,

$$(A.13) \quad \lim_{M \rightarrow \infty} \lim_{a \rightarrow \infty} \mathbb{E} \left[(\text{the 3rd term on the RHS of (A.2)})^2 \middle| \mathcal{Y}_{t_{i+1}} \right] = 0,$$

for any bounded ϕ .

Error caused by artificial evolution: By [\(A.10\)](#) in [Remark 3.3](#), we can conclude that for any ϕ satisfies the requirement in [Theorem 3.8](#), there holds

$$(A.14) \quad \lim_{M \rightarrow \infty} \lim_{a \rightarrow \infty} \mathbb{E} \left[(\text{the 2nd term on the RHS of (A.2)})^2 \middle| \mathcal{Y}_{t_{i+1}} \right] = 0.$$

Error caused by finite sampling: For any ϕ satisfying the requirement in [Theorem 3.8](#), the relations [\(A.12\)](#), [\(A.13\)](#), [\(A.14\)](#), and [\(A.11\)](#) (for the integer i) imply

$$(A.15) \quad \lim_{M \rightarrow \infty} \lim_{a \rightarrow \infty} \mathbb{E} \left[\left| \hat{\pi}_{M,t_i} (K_{\Delta t_i} \ell_{Y(t_{i+1})} \phi) - \pi_{M,t_{i+1}} (K_{\Delta t_i}^{N,\gamma_1} \ell_{Y(t_{i+1})} \phi) \right|^2 \middle| \mathcal{Y}_{t_{i+1}} \right] = 0.$$

Therefore, to analyze the error caused by finite sampling, we only need to compare $\bar{\pi}_{M,t_i}(\phi)$ and $\frac{\hat{\pi}_{M,t_{i+1}}(K_{\Delta t_i} \ell_{Y(t_{i+1})} \phi)}{\hat{\pi}_{M,t_{i+1}}(K_{\Delta t_i} \ell_{Y(t_{i+1})} \phi)}$. For any function ϕ satisfying the requirement in [Theorem 3.8](#), we define

$$\bar{\rho}_{M,t_{i+1}}(\phi) = \sum_{j=1}^M \phi(\kappa_j(t_{i+1}), x_j(t_{i+1})) \quad \forall i \in \mathbb{N},$$

which is the estimate of the function ϕ right before the collection of $Y(t_{i+1})$. Since the increments of the particles in the sampling step are independent, this quantity satisfies

$$(A.16) \quad \mathbb{E} \left[\left| \bar{\rho}_{M,t_{i+1}}(\phi) - \hat{\pi}_{M,t_{i+1}} (K_{\Delta t_i}^{N,\gamma_1} \ell_{Y(t_{i+1})} \phi) \right|^2 \middle| \mathcal{Y}_{t_{i+1}} \right] \leq \frac{\|\ell_{Y(t_{i+1})} \phi\|_\infty^2}{M}.$$

Moreover, by [9, (2.10)], there is

$$\begin{aligned} & \left| \bar{\pi}_{M,t_{i+1}}(\phi) - \frac{\tilde{\pi}_{M,t_{i+1}}(K_{\Delta t_i} \ell_{Y(t_{i+1})} \phi)}{\tilde{\pi}_{M,t_{i+1}}(K_{\Delta t_i} \ell_{Y(t_{i+1})})} \right| \\ & \leq \frac{\|\phi\|_\infty}{\tilde{\pi}_{M,t_{i+1}}(K_{\Delta t_i} \ell_{Y(t_{i+1})})} \left| \bar{\rho}_{M,t_{i+1}}(\ell_{y_{i+1}}) - \tilde{\pi}_{M,t_{i+1}}(K_{\Delta t_i} \ell_{Y(t_{i+1})}) \right| \\ & \quad + \frac{1}{\tilde{\pi}_{M,t_{i+1}}(K_{\Delta t_i} \ell_{Y(t_{i+1})})} \left| \bar{\rho}_{M,t_{i+1}}(\ell_{y_{i+1}} \phi) - \tilde{\pi}_{M,t_{i+1}}(K_{\Delta t_i} \ell_{Y(t_{i+1})} \phi) \right|. \end{aligned}$$

Recall that the likelihood function $\ell_{Y(t_{i+1})}$ has a $\mathcal{Y}_{t_{i+1}}$ measurable, positive lower bound due to the boundedness of $h(\cdot)$, so $\tilde{\pi}_{M,t_{i+1}}(K_{\Delta t_i} \ell_{Y(t_{i+1})})$ is also greater than or equal to this bound. Thus, by applying (A.16) to this inequality, we have

$$\lim_{M \rightarrow \infty} \lim_{a \rightarrow 0} \mathbb{E} \left[\left(\bar{\pi}_{M,t_{i+1}}(\phi) - \frac{\tilde{\pi}_{M,t_{i+1}}(K_{\Delta t_i} \ell_{Y(t_{i+1})} \phi)}{\tilde{\pi}_{M,t_{i+1}}(K_{\Delta t_i} \ell_{Y(t_{i+1})})} \right)^2 \middle| \mathcal{Y}_{t_{i+1}} \right] = 0,$$

which together with (A.15) suggest the error caused by finite sampling is controlled, i.e.,

$$(A.17) \quad \lim_{M \rightarrow \infty} \lim_{a \rightarrow \infty} \mathbb{E} [(\text{the 1st term on the RHS of (A.2)})^2 | \mathcal{Y}_{t_{i+1}}] = 0.$$

Finally, by applying (A.12), (A.13), (A.14), and (A.17) to (A.2), we can conclude that if (A.11) holds for a positive integer i , then it also holds for the positive integer $i + 1$, which proves the result. \square

REFERENCES

- [1] D. F. ANDERSON, *Incorporating postleap checks in tau-leaping*, The Journal of chemical physics, 128 (2008), p. 054103.
- [2] D. F. ANDERSON, A. GANGULY, T. G. KURTZ, ET AL., *Error analysis of tau-leap simulation methods*, The Annals of Applied Probability, 21 (2011), pp. 2226–2262.
- [3] D. F. ANDERSON AND T. G. KURTZ, *Continuous time markov chain models for chemical reaction networks*, in Design and analysis of biomolecular circuits, Springer, 2011, pp. 3–42.
- [4] S. K. AOKI, G. LILLACCI, A. GUPTA, A. BAUMSCHLAGER, D. SCHWEINGRUBER, AND M. KHAMMASH, *A universal biomolecular integral feedback controller for robust perfect adaptation*, Nature, 570 (2019), pp. 533–537.
- [5] A. BAIN AND D. CRISAN, *Fundamentals of stochastic filtering*, vol. 60, Springer Science & Business Media, 2008.
- [6] C. BERZUINI AND W. GILKS, *Resample-move filtering with cross-model jumps*, in Sequential Monte Carlo Methods in Practice, Springer, 2001, pp. 117–138.
- [7] C. BRIAT, A. GUPTA, AND M. KHAMMASH, *Antithetic integral feedback ensures robust perfect adaptation in noisy biomolecular networks*, Cell systems, 2 (2016), pp. 15–26.
- [8] Y. CAO, D. T. GILLESPIE, AND L. R. PETZOLD, *Efficient step size selection for the tau-leaping simulation method*, The Journal of chemical physics, 124 (2006), p. 044109.
- [9] D. CRISAN, *Particle filters—a theoretical perspective*, in Sequential Monte Carlo methods in practice, Springer, 2001, pp. 17–41.
- [10] D. CRISAN, J. MÍGUEZ, ET AL., *Particle-kernel estimation of the filter density in state-space models*, Bernoulli, 20 (2014), pp. 1879–1929.
- [11] A. CRUDU, A. DEBUSSCHE, AND O. RADULESCU, *Hybrid stochastic simplifications for multiscale gene networks*, BMC systems biology, 3 (2009), p. 89.
- [12] F. DAUM AND J. HUANG, *Particle flow for nonlinear filters with log-homotopy*, in Signal and Data Processing of Small Targets 2008, vol. 6969, International Society for Optics and Photonics, 2008, p. 696918.
- [13] P. DEL MORAL AND L. MICLO, *Branching and interacting particle systems approximations of feynman-kac formulae with applications to non-linear filtering*, in Seminaire de probabilites XXXIV, Springer, 2000, pp. 1–145.
- [14] A. DOUCET AND A. M. JOHANSEN, *A tutorial on particle filtering and smoothing: Fifteen years later*, Handbook of nonlinear filtering, 12 (2009), p. 3.

- [15] A. DUNCAN, R. ERBAN, AND K. ZYGALAKIS, *Hybrid framework for the simulation of stochastic chemical kinetics*, Journal of Computational Physics, 326 (2016), pp. 398–419.
- [16] D. FALLER, U. KLINGMÜLLER, AND J. TIMMER, *Simulation methods for optimal experimental design in systems biology*, Simulation, 79 (2003), pp. 717–725.
- [17] Z. FANG, A. GUPTA, AND M. KHAMMASH, *Stochastic filtering for multiscale stochastic reaction networks based on hybrid approximations*, arXiv:2106.03276 [q-bio.QM].
- [18] ———, *Stochastic filters based on hybrid approximations of multiscale stochastic reaction networks*, in 2020 59th IEEE Conference on Decision and Control (CDC), IEEE, 2020, pp. 4616–4621.
- [19] M. A. GIBSON AND J. BRUCK, *Efficient exact stochastic simulation of chemical systems with many species and many channels*, The journal of physical chemistry A, 104 (2000), pp. 1876–1889.
- [20] W. R. GILKS AND C. BERZUINI, *Following a moving target—monte carlo inference for dynamic bayesian models*, Journal of the Royal Statistical Society: Series B (Statistical Methodology), 63 (2001), pp. 127–146.
- [21] D. T. GILLESPIE, *A general method for numerically simulating the stochastic time evolution of coupled chemical reactions*, Journal of computational physics, 22 (1976), pp. 403–434.
- [22] ———, *Exact stochastic simulation of coupled chemical reactions*, The journal of physical chemistry, 81 (1977), pp. 2340–2361.
- [23] ———, *The chemical langevin equation*, The Journal of Chemical Physics, 113 (2000), pp. 297–306.
- [24] ———, *Approximate accelerated stochastic simulation of chemically reacting systems*, The Journal of chemical physics, 115 (2001), pp. 1716–1733.
- [25] A. GOLIGHTLY AND D. J. WILKINSON, *Bayesian sequential inference for stochastic kinetic biochemical network models*, Journal of Computational Biology, 13 (2006), pp. 838–851.
- [26] N. J. GORDON, D. J. SALMOND, AND A. F. SMITH, *Novel approach to nonlinear/non-gaussian bayesian state estimation*, in IEE proceedings F (radar and signal processing), vol. 140, IET, 1993, pp. 107–113.
- [27] A. GUPTA AND M. KHAMMASH, *Unbiased estimation of parameter sensitivities for stochastic chemical reaction networks*, SIAM Journal on Scientific Computing, 35 (2013), pp. A2598–A2620.
- [28] ———, *Sensitivity analysis for multiscale stochastic reaction networks using hybrid approximations*, Bulletin of Mathematical Biology, 81 (2019), pp. 3121–3158.
- [29] A. GUPTA, M. RATHINAM, AND M. KHAMMASH, *Estimation of parameter sensitivities for stochastic reaction networks using tau-leap simulations*, SIAM Journal on Numerical Analysis, 56 (2018), pp. 1134–1167.
- [30] B. HEPP, A. GUPTA, AND M. KHAMMASH, *Adaptive hybrid simulations for multiscale stochastic reaction networks*, The Journal of chemical physics, 142 (2015), p. 034118.
- [31] K. L. HEY, H. MOMIJI, K. FEATHERSTONE, J. R. DAVIS, M. R. WHITE, D. A. RAND, AND B. FINKENSTÄDT, *A stochastic transcriptional switch model for single cell imaging data*, Biostatistics, 16 (2015), pp. 655–669.
- [32] Y. HU, T. LI, AND B. MIN, *The weak convergence analysis of tau-leaping methods: revisited*, Communications in Mathematical Sciences, 9 (2011), pp. 965–996.
- [33] R. E. KALMAN, *A new approach to linear filtering and prediction problems*, (1960).
- [34] H.-W. KANG, T. G. KURTZ, ET AL., *Separation of time-scales and model reduction for stochastic reaction networks*, The Annals of Applied Probability, 23 (2013), pp. 529–583.
- [35] H.-W. KANG, T. G. KURTZ, L. POPOVIC, ET AL., *Central limit theorems and diffusion approximations for multiscale markov chain models*, The Annals of Applied Probability, 24 (2014), pp. 721–759.
- [36] N. KANTAS, A. DOUCET, S. S. SINGH, J. MACIEJOWSKI, N. CHOPIN, ET AL., *On particle methods for parameter estimation in state-space models*, Statistical science, 30 (2015), pp. 328–351.
- [37] F. LE GLAND, N. OUDJANE, ET AL., *Stability and uniform approximation of nonlinear filters using the hilbert metric and application to particle filters*, The Annals of Applied Probability, 14 (2004), pp. 144–187.
- [38] T. LI, *Analysis of explicit tau-leaping schemes for simulating chemically reacting systems*, Multiscale Modeling & Simulation, 6 (2007), pp. 417–436.
- [39] J. LIU AND M. WEST, *Combined parameter and state estimation in simulation-based filtering*, in Sequential Monte Carlo methods in practice, Springer, 2001, pp. 197–223.
- [40] X. LIU AND M. NIRANJAN, *State and parameter estimation of the heat shock response system using kalman and particle filters*, Bioinformatics, 28 (2012), pp. 1501–1507.
- [41] J. C. LOCKE AND M. B. ELWITZ, *Using movies to analyse gene circuit dynamics in single cells*, Nature Reviews Microbiology, 7 (2009), pp. 383–392.

- [42] H. H. McADAMS AND A. ARKIN, *Stochastic mechanisms in gene expression*, Proceedings of the National Academy of Sciences, 94 (1997), pp. 814–819.
- [43] K. MURPHY AND S. RUSSELL, *Rao-blackwellised particle filtering for dynamic bayesian networks*, in Sequential Monte Carlo methods in practice, Springer, 2001, pp. 499–515.
- [44] N. OUDJANE AND C. MUSSO, *Progressive correction for regularized particle filters*, in Proceedings of the Third International Conference on Information Fusion, vol. 2, IEEE, 2000, pp. THB2–10.
- [45] M. RATHINAM, *Convergence of moments of tau leaping schemes for unbounded markov processes on integer lattices*, SIAM Journal on Numerical Analysis, 54 (2016), pp. 415–439.
- [46] M. RATHINAM, L. R. PETZOLD, Y. CAO, AND D. T. GILLESPIE, *Stiffness in stochastic chemically reacting systems: The implicit tau-leaping method*, The Journal of Chemical Physics, 119 (2003), pp. 12784–12794.
- [47] ———, *Consistency and stability of tau-leaping schemes for chemical reaction systems*, Multi-scale Modeling & Simulation, 4 (2005), pp. 867–895.
- [48] M. RATHINAM AND M. YU, *State and parameter estimation from exact partial state observation in stochastic reaction networks*, The Journal of Chemical Physics, 154 (2021), p. 034103.
- [49] N. ROSENFELD, J. W. YOUNG, U. ALON, P. S. SWAIN, AND M. B. ELOWITZ, *Gene regulation at the single-cell level*, science, 307 (2005), pp. 1962–1965.
- [50] M. RULLAN, D. BENZINGER, G. W. SCHMIDT, A. MILIAS-ARGEITIS, AND M. KHAMMASH, *An optogenetic platform for real-time, single-cell interrogation of stochastic transcriptional regulation*, Molecular cell, 70 (2018), pp. 745–756.
- [51] D. SCHNOERR, G. SANGUINETTI, AND R. GRIMA, *Approximation and inference methods for stochastic biochemical kinetics—a tutorial review*, Journal of Physics A: Mathematical and Theoretical, 50 (2017), p. 093001.
- [52] C. SHERLOCK, A. GOLIGHTLY, AND C. S. GILLESPIE, *Bayesian inference for hybrid discrete-continuous stochastic kinetic models*, Inverse Problems, 30 (2014), p. 114005.
- [53] S. SONG, G.-S. YANG, S. J. PARK, S. HONG, J.-H. KIM, AND J. SUNG, *Frequency spectrum of chemical fluctuation: A probe of reaction mechanism and dynamics*, PLoS computational biology, 15 (2019), p. e1007356.
- [54] D. J. STEPHENS AND V. J. ALLAN, *Light microscopy techniques for live cell imaging*, science, 300 (2003), pp. 82–86.
- [55] S. C. SURACE, A. KUTSCHIREITER, AND J.-P. PFISTER, *How to avoid the curse of dimensionality: Scalability of particle filters with and without importance weights*, SIAM review, 61 (2019), pp. 79–91.
- [56] N. G. VAN KAMPEN, *The expansion of the master equation*, Adv. Chem. Phys, 34 (1976), pp. 245–309.
- [57] C. VONESCH, F. AGUET, J.-L. VONESCH, AND M. UNSER, *The colored revolution of bioimaging*, IEEE signal processing magazine, 23 (2006), pp. 20–31.
- [58] J. YANG, V. KADIRKAMANATHAN, AND S. A. BILLINGS, *In vivo intracellular metabolite dynamics estimation by sequential monte carlo filter*, in 2007 IEEE Symposium on Computational Intelligence and Bioinformatics and Computational Biology, IEEE, 2007, pp. 387–394.
- [59] T. YANG, P. G. MEHTA, AND S. P. MEYN, *Feedback particle filter*, IEEE transactions on Automatic control, 58 (2013), pp. 2465–2480.
- [60] C. ZECHNER, M. UNGER, S. PELET, M. PETER, AND H. KOEPL, *Scalable inference of heterogeneous reaction kinetics from pooled single-cell recordings*, Nature methods, 11 (2014), pp. 197–202.
- [61] J. ZHANG, R. E. CAMPBELL, A. Y. TING, AND R. Y. TSIEN, *Creating new fluorescent probes for cell biology*, Nature reviews Molecular cell biology, 3 (2002), pp. 906–918.